Title

RNAs interact with BRD4 to promote enhanced chromatin engagement and transcription activation

Journal

Nature Structural & Molecular Biology, 25(8)

ISSN

1545-9993

Authors

Rahnamoun, Homa
Lee, Jihoon
Sun, Zhengxi
et al.

Publication Date

2018-08-01

DOI

10.1038/s41594-018-0102-0

Peer reviewed

RNAs Interact with BRD4 to Promote Enhanced Chromatin Engagement and Transcription Activation

Homa Rahnamoun[1], Jihoon Lee[1], Zhengxi Sun[1], Hanbin Lu[1], Kristen M. Ramsey[2], Elizabeth A. Komives[2], and Shannon M. Lauberth[1]*

[1] Section of Molecular Biology, University of California, San Diego, 9500 Gilman Drive, La Jolla, CA 92093, USA

[2] Department of Chemistry and Biochemistry, University of California, San Diego, 9500 Gilman Drive, La Jolla, CA 92093, USA

*Correspondence: slauberth@ucsd.edu

Abstract

Bromodomain and extra-terminal domain (BET) BRD4 binds to acetylated histones at enhancers and promoters through conserved bromodomains (BDs) to function as a master regulator of transcriptional elongation. Here, we reveal through global profiling analysis, an extensive recruitment of BRD4 at active enhancers that are co-occupied by mutant p53 and support the synthesis of enhancer-directed (eRNA) transcripts in response to chronic immune signaling. We identify that BRD4 is a highly robust binding module for RNAs and that there exists marked selectivity of BRD4 associations with eRNAs that are produced from enhancers bound by BRD4. Through biochemical and biophysical characterizations, we show that BRD4 BDs function cooperatively as docking sites for eRNAs and that the BDs of BRD2, BRD3, BRDT, BRG1, and BRD7 also interact directly with eRNAs. BRD4-eRNA interactions increase BRD4 binding to acetylated histones and promote enhanced BRD4 recruitment at specific enhancers that in turn augments BRD4 transcriptional activities. This work provides a previously unrecognized convergence between eRNAs and histone posttranslational modifications in regulating BRD4 binding and highlights a mechanism by which eRNAs play a direct

role in gene regulation by modulating enhancer interactions and transcriptional functions of BRD4.

Main

Enhancers shape gene expression programs that drive cellular processes by acting to coalesce information from environmental stimuli and the coordinated activities of multiple transcription factors and cofactors[1-5]. Our ability to predict and annotate enhancers and their activity states across multiple cell and tissue types stems from the identification of distinct epigenomic signatures that include an accumulation of the histone marks, histone H3 lysine 4 monomethylation (H3K4me1) that together with histone H3 lysine 27 acetylation (H3K27ac) demarcates active enhancers[3,6,7-9]. Histone lysine acetylation plays a critical role in the context of chromatin, most generally by contributing to chromatin accessibility and transcriptional activation[10]. A diverse number of transcriptional coregulators and chromatin modifying enzymes bind to acetylated histones through bromodomain (BD) modules, particularly at active enhancers[11]. The affinity and selectivity of BD interactions with acetylated lysine residues are typically weak in nature, but can be increased by BD interactions with multiple and neighboring acetylation sites within the histone tail[12-14], suggesting that additional mechanisms regulating BD binding at enhancers are likely to have important implications for chromatin regulation and transcription.

The bromodomain and extraterminal motif (BET) proteins are among the well-known proteins that bind to histone acetylation through their tandem amino-terminal BDs (BD1 and BD2)[11,15]. BRD4, a well-studied member of the BET family binds to acetylated histones and non-histone proteins at enhancers and promoters[11,16-18] to regulate gene expression programs that play particularly pivotal roles in inflammation and cancer development[19-21]. BRD4 has been shown to associate with multiple transcriptional regulators, that include TWIST, p53, C/EBPα, C/EBPβ, ERG, and NFκB, which has provided increasing support of its role in

enhancer and gene regulation[22-28]. Most recently, BRD4 enhancer binding was shown to modulate gene expression to control cellular identity during adipogenesis and myogenesis[29]. Highly selective inhibitors of the BET family including JQ1 have demonstrated that BRD4 binding at enhancers supports eRNA production[30] and super-enhancer formation[31-33]. In addition, BRD4 promotes RNAPII elongation at enhancers and within protein-coding genes through its recruitment of the active form of Positive Elongation Factor-b (P-TEFb)[34,35] and by its ability to exhibit histone chaperone activity to overcome nucleosomal barriers for elongating RNAPII[36]. While there are clear links between BRD4 and context-dependent gene regulation, the molecular mechanisms underlying the enhancer and gene-specific targeting and functions of BRD4 remain elusive.

The widespread synthesis of eRNAs that is regulated by transcriptional cofactors such as BRD4 serves as a measure of enhancer activity and has been implicated in the regulation of gene expression in multiple cell types and in response to different stimuli[37,38]. Various roles of eRNAs have stemmed from recent studies linking eRNAs to enhancer-promoter interaction interfaces[39,40], chromatin remodeling[41], the release of paused RNAPII[42], and the recruitment of general cofactors that include cohesin[39,40], Mediator[41,43], and the histone acetyltransferase CBP[44]. While eRNAs are well positioned to dynamically remodel cellular transcriptomes and add a new layer of complexity to gene regulation, the molecular basis by which eRNAs function in enhancer and gene regulation, and their connection with other epigenetic features at active enhancers remain poorly understood.

In this study, we show that RNAs directly interact with the BDs of BRD4, and that similar RNA interactions exist for the BDs of all BET family members and non-BET proteins, BRG1 and BRD7. Notably, we find that eRNAs exhibit cooperativity with acetylated histone lysines *in vitro* and at active enhancers to augment BRD4 binding and transcriptional activity. Collectively, our results provide evidence for a feedforward

epigenetic mechanism in which eRNAs through direct interactions with BRD4 support an active enhancer landscape that modulates proinflammatory gene expression.

Results

BRD4 binds and functions at p53 R273H bound enhancers in response to chronic TNF-α signaling

Since BRD4 has been shown to occupy and regulate enhancer function[33,45-47], we sought to investigate whether BRD4 regulates recently identified signal-dependent enhancers that are activated by mutant p53 in response to chronic immune signaling[48]. Using genome-wide chromatin immunoprecipitation followed by sequencing (ChIP-seq) in human SW480 colon cancer cells, expressing the hotspot mutant p53 R273H (hereafter mutp53) and treated with tumor necrosis factor alpha (TNF-α) for 16 hr, we identified stringent BRD4 binding peaks (n=21,528, p-value < 10^{-5}). Comparative analyses of the BRD4 binding peaks with our previously published mutp53, H3K4me1, and H3K27ac ChIP-seq data in response to chronic TNF-α signaling[48] showed a striking colocalization of BRD4 binding peaks with the peak sites for mutp53 and the histone marks H3K4me1 and H3K27ac, which demarcate active enhancers (Fig. 1a). Specifically, we identified that approximately a third (28%, n=5,949, p-value < 10^{-5}) of the total BRD4 binding sites occur at intergenic sites overlapping with active enhancers (Supplementary Fig. 1a). Remarkably, over 80% (n= 4,884, p-value < 10^{-5}) of the BRD4 binding sites that overlap with active enhancers are also occupied by mutp53 (Supplementary Fig. 1a). Furthermore, *de novo* motif analysis identified that NFκB/p65 and EWS:ERG fusion (ETS) consensus motifs are among the most highly enriched motifs to overlap with the BRD4 and mutp53 peaks (Supplementary Fig. 1b). This analysis is consistent with our previous findings that NFκB plays a significant role in the recruitment of mutp53 at active enhancers in response to chronic immune signaling[48]. To investigate whether mutp53 and BRD4 simultaneously bind active enhancers in response to TNF-α-

signaling, sequential ChIP was performed and the precipitated DNA was analyzed by quantitative PCR (qPCR) using primer sets designed against the enhancer (amplicon A) and downstream control (amplicon B) regions of the *MMP9* and *CCL2* enhancers, which are among the signal-dependent enhancers that we recently found to be bound and activated by mutp53 and NFκB in response to chronic TNF-α signaling[48]. In response to chronic TNF-α signaling, selective and simultaneous binding of mutp53 and BRD4 was observed at the *MMP9* and *CCL2* enhancers, but not the control regions (Supplementary Fig. 1c). We also identified that BRD4 and mutp53 form comparable physiological associations in SW480 cells before and following TNF-α treatment as revealed by co-immunoprecipitation (Co-IP) analyses with an antibody specific to BRD4 (Supplementary Fig. 1d). Using purified proteins, we also revealed that BRD4 forms direct interactions with mutp53 and wild-type (WT) p53 (Supplementary Fig. 1e), which is similar to previous reports revealing an interaction between BRD4 and WT p53[24]. We next assessed whether mutp53 contributes to BRD4 binding at enhancers by performing ChIP-qPCR analyses in SW480 cells expressing doxycycline-inducible short hairpin RNAs (shRNAs) against mutp53 following TNF-α treatment for 16 hr. Relative to a non-targeting shRNA against LacZ (Ctrl), p53 shRNA markedly reduced mutp53 protein levels after TNF-α treatment without affecting BRD4 protein levels (Supplementary Fig. 1f). As shown in Fig. 1b, mutp53 knockdown resulted in a comparable loss (approximately 66% and 72%) of mutp53 binding at the *MMP9* and *CCL2* enhancer regions, respectively. Notably, this decrease in mutp53 binding resulted in a significant reduction in BRD4 binding at the *MMP9* (52%) and *CCL2* (65%) enhancers (Fig. 1b). Together, these results establish functional mutp53-BRD4 interactions that are consistent with the colocalization of mutp53 and BRD4 across the genome and further underscore the requirement for mutp53 in regulating BRD4 binding at active enhancers in response to chronic TNF-α signaling.

To determine whether BRD4 contributes to the regulation of BRD4 and mutp53 co-bound enhancers, we next examined the global levels of nascent transcription (+/- TNF-α) centered upon the enhancer-specific BRD4 and mutp53 ChIP-seq peaks using our global run-on sequencing (GRO-seq) data[48]. As revealed in Fig. 1c, markedly induced eRNA levels following 16 hr TNF-α treatment were identified at H3K27ac-enriched intergenic sites that are co-occupied by BRD4 and mutp53. Notably, the TNF-induced eRNA levels observed at the mutp53 and BRD4 co-bound enhancers were significantly higher relative to eRNA levels at H3K27ac-enriched intergenic sites that were not co-bound by BRD4 and mutp53 and in response to chronic TNF signaling. To examine a direct role for BRD4 in the regulation of TNF-α-induced enhancer transcription, we established SW480 cells stably expressing nontargeting (Ctrl) or two different shRNA oligonucleotides specific to BRD4 (BRD4-1 and BRD4-2). As shown in Fig. 1d, relative to the control knockdown, both shRNAs against BRD4 significantly and comparably decreased BRD4 mRNA and protein levels. ChIP-qPCR analyses in control knockdown cells (+/- TNF-α) revealed that BRD4 binding at the active enhancers adjacent to the *MMP9* and *CCL2* gene loci is significantly increased (53% and 70%, respectively) in response to chronic TNF-α signaling (Fig. 1e). As expected, BRD4 knockdown resulted in a significant loss in TNF-α-inducible BRD4 binding that occurs at the *MMP9* and *CCL2* enhancers (55% and 63%, respectively) (Fig. 1e). Notably, this decrease in TNF-α-induced BRD4 binding resulted in a significant loss in the TNF-α-inducible eRNA levels of *MMP9* and *CCL2* (four-fold and six-fold, respectively) and a comparable (two-fold) decrease in the TNF-α-induced mRNA levels of both *MMP9* and *CCL2* (Fig. 1f; Supplementary Fig. 1g). In comparison, under uninduced conditions, little to no effect on BRD4 binding and eRNA/mRNA expression levels was identified at the *MMP9* and *CCL2* enhancers following BRD4 shRNA-mediated knockdown (Figs. 1e,f; Supplementary Fig. 1g). The significant reduction in the TNF-α-induced *MMP9* and *CCL2* eRNA and mRNA

expression levels following BRD4 knockdown was found to be independent of a decrease in mutp53 binding at the *MMP9* and *CCL2* enhancers (Supplementary Fig. 1h). This data, taken together with our mutp53 shRNA-mediated knockdown data, which revealed a significant loss in TNF-α-induced BRD4 binding at the *MMP9* and *CCL2* enhancers (Fig. 1b), demonstrates that while mutp53 is required for BRD4 binding, BRD4 is not required to support mutp53 at this subset of enhancers. Consistent with our results following shRNA-mediated BRD4 knockdown (Fig. 1f; Supplementary Fig. 1g), treatment of SW480 cells with the BET inhibitor, JQ1[45], which did not affect BRD4 protein levels (Supplementary Fig. 1i), resulted in a significant decrease in the TNF-α-inducible *MMP9* and *CCL2* eRNA and mRNA levels. This identified role for BRD4 in regulating the TNF-induced expression of eRNAs and tumor promoting genes is consistent with our previous observations revealing that mutp53 is also required to support TNF-α-inducible eRNA/mRNA expression levels in SW480 colon cancer cells[48]. Collectively, these data strongly suggest that BRD4 acts coordinately with mutp53 at active enhancers to support potent levels of eRNA synthesis and nearby gene expression in response to chronic TNF-α signaling.

BRD4 associates with RNAs synthesized from genomic regions occupied by BRD4

Given the significant overlap between BRD4 enrichment and potent eRNA synthesis in response to chronic TNF-α signaling and the previously described association of BRD4 with RNAPII elongation complexes[36], we examined whether BRD4 associates with RNAs under physiological conditions by performing UV-crosslinked RNA immunoprecipitation (UV-RIP) in SW480 cells (+/- TNF-α). BRD4 mRNA and protein levels were found to be unaffected by chronic TNF-α treatment in this cell line (Supplementary Fig. 2a). In TNF-α-treated SW480 cells, we found that a BRD4 antibody specifically co-immunoprecipitated eRNAs produced from the *MMP9*, *CCL2*, *CSF2*, and *TNFAIP3* but not the *TFAP2A* and *MPP7* enhancers (Fig. 2a; Supplementary Fig. 2b) despite that the *TFAP2A* and *MPP7*

eRNAs were expressed at comparable or even higher levels relative to the *MMP9*, *CCL2*, *CSF2*, and *TNFAIP3* eRNAs as revealed by our GRO-seq data (Fig. 2c; Supplementary Fig. 2c). We also found that BRD4 associates with *MMP9* and *CCL2* mRNAs but not the *TFAP2A* and *MPP7* mRNAs in response to chronic TNF-α signaling (Fig. 2b). In comparison, under uninduced conditions, BRD4 was not found to associate with any of the examined *MMP9*, *CCL2*, *TFAP2A*, *MPP7*, *CSF2*, and *TNFAIP3* RNAs (Figs. 2a,b; Supplementary Fig. 2b). The specific association of BRD4 with RNAs in response to chronic TNF-α signaling is consistent with the significantly higher expression levels of these RNAs in the TNF-α-induced versus uninduced cells as demonstrated by our GRO-seq data (Fig. 2c; Supplementary Fig. 2c). Notably, BRD4-RNA associations are also consistent with BRD4 binding levels, which were found to be significantly higher at the *MMP9* and *CCL2* relative to the *TFAP2A* and *MPP7* enhancers and transcription start sites (TSSs) in response to chronic TNF-α signaling as demonstrated by our BRD4 ChIP-seq data (Fig. 2d). Also consistent, is the identification that the TNF-α-induced associations of BRD4 with the *CSF2* and *TNFAIP3* eRNAs (Supplementary Fig. 2b) parallels with the high levels of BRD4 binding at the *CSF2* and *TNFAIP3* enhancers (Supplementary Fig. 2c).

Having identified a physiological association between BRD4 and RNAs that are produced from genomic regions occupied by BRD4 in response to chronic TNF-α signaling, we next examined whether recombinant BRD4 full-length (FL) directly interacts with *in vitro* transcribed eRNAs, as well as several other RNA molecules including long noncoding RNAs (lncRNAs) and exonic RNAs. Consistent with our UV-RIP analyses in SW480 cells, we identified that BRD4 interacts directly with the *MMP9* and *CCL2* eRNAs (Supplementary Fig. 2d). In addition, we also found that BRD4 directly interacts with the *MEG3* lncRNA and the *p21* exonic RNA (Supplementary Fig. 2d). Together with our UV-RIP analyses, these findings suggest that BRD4 displays broad rather than sequence-specific RNA interactions

and that BRD4-eRNA associations occur in an enhancer- and locus-specific manner such that BRD4 associates with specific RNAs synthesized from genomic regions that are significantly enriched for BRD4 binding in response to chronic TNF-α signaling.

BRD4 directly interacts with eRNAs through its tandem bromodomains

Having established physiological and direct interactions between BRD4 and RNAs, we further investigated the direct binding of BRD4 to eRNAs. RNA electrophoretic mobility shift assays (EMSAs) were performed using purified BRD4 FL and a ^{32}P-labeled *MMP9* eRNA probe. As revealed in Fig. 3a, we observed the formation of a single prominent BRD4-*MMP9* eRNA complex. Quantification of the RNA EMSA with increasing doses of BRD4 FL revealed that ~80% of the *MMP9* eRNA was bound by BRD4 FL at the highest titration of BRD4 FL protein (Supplementary Fig. 2e). To further test the specificity of BRD4-*MMP9* eRNA interactions, competition EMSAs were performed in the presence of increasing amounts of unlabeled *CCL2* eRNA or a single strand *MMP9* DNA probe. BRD4 binding to the labeled *MMP9* eRNA probe was specifically competed by excess amounts of cold *CCL2* eRNA (Fig. 3b). In comparison, identical amounts of the *MMP9* ssDNA were significantly less efficient in competing BRD4-*MMP9* eRNA interactions (Fig. 3b), which demonstrates that BRD4 binds preferentially to RNA sequences *in vitro*.

To identify the specific domains of BRD4 that contribute to interactions with eRNAs, we next performed RNA pulldown assays using BRD4 deletion mutants (Fig. 3c) and *in vitro* transcribed *MMP9* and *CCL2* eRNAs. Both recombinant BRD4 FL and the naturally existing short BRD4 isoform spanning from amino acids 1-722[49] bind strongly and comparably to the *MMP9* and *CCL2* eRNAs (Fig. 3d). Next, we tested the contributions of the BRD4 bromodomains (BDs) since these chromatin interacting domains localize within the eRNA interacting BRD4 (1-722) protein. As revealed by RNA pulldown assays, a truncated form of BRD4 that is devoid of both BDs (Fig. 3c, BRD4 ΔBD1/2) showed a nearly complete loss of

binding to the *MMP9* and *CCL2* eRNAs (Fig. 3d). Similarly, RNA EMSAs revealed that radiolabeled *MMP9* eRNA did not display a robust mobility shift when titrated with BRD4 ΔBD1/2 as compared to BRD4 FL (Fig. 3e). Specifically, we found that less than 5% relative to the nearly 80% of the labeled eRNA was bound by BRD4 ΔBD1/2 as compared to BRD4 FL, respectively (Fig. 3e; Supplementary Fig. 2e). Together, the RNA pulldown assays and EMSA experiments reveal a requirement for the BDs in facilitating BRD4-eRNA interactions.

We next tested whether the individual BRD4 BDs (Fig. 3c, BD1 or BD2) are sufficient to support BRD4-eRNA interactions by expressing and purifying the isolated BD1 and BD2 domains. Notably, we found that neither BD1 nor BD2 are able to bind RNA as strongly as the BRD4 (1-722) protein as revealed by the significant decrease in their interactions with the *MMP9* and *CCL2* eRNAs (Fig. 3f). To further verify whether BD1 and BD2 are both required for eRNA interactions, we expressed and purified a longer BRD4 protein (Fig. 3c; BRD4 BD1/2) consisting of both BDs and the linker sequence that joins BD1 and BD2, which revealed a level of eRNA binding that is comparable to BRD4 (1-722) (Fig. 3f). To expand upon the contributions of other BDs in facilitating eRNA interactions, we tested the BDs of additional BET family members, BRD2, BRD3, and BRDT as well as non-BET proteins, BRG1 and BRD7. As shown in Fig. 3g, the tandem BDs (BD1/2) of BRD2, BRD3, BRD4, BRDT, and the single BDs of BRG1 and BRD7 bind to *MMP9* and *CCL2* eRNAs with the eRNA interaction levels of BRG1 and BRDT relatively lower as compared to the other BD-containing proteins. Taken together, these findings demonstrate that BDs directly interact with eRNAs and that the tandem BRD4 BDs function cooperatively to facilitate BRD4-eRNA interactions.

eRNAs enhance BRD4 binding to acetylated histone H3 and H4 peptides and reconstituted histone octamers

Having identified that eRNAs bind to the BRD4 BDs, which are known to support BRD4 interactions with acetylated lysines[50,51], we next investigated the significance of eRNA-BRD4 interactions in the regulation of BRD4 binding to acetylated histones. First, *in vitro* binding assays were performed with K27ac-modified histone H3, K16ac-modified histone H4, or unmodified H3/H4 peptides. As expected, BRD4 FL (Figs. 4a,b lane 7 versus 3), but not BRD4 ΔBD1/2 (Figs. 4a,b lane 9 versus 5) bound more strongly to H3K27ac- and H4K16ac-modified versus unmodified peptides. Notably, the binding of BRD4 FL to acetylated H3K27 and H4K16 peptides was significantly increased in the presence of *MMP9* eRNA (Figs. 4a,b lane 8 versus 7). In addition, eRNAs were not found to promote BRD4 binding in the absence of BRD4 interactions with acetylated peptides, as demonstrated by the inability of eRNAs to support BRD4 FL binding to unmodified histone H3 and H4 peptides (Figs. 4a,b lane 4 versus 3) and the lack of an eRNA effect on BRD4 ΔBD1/2 binding to acetylated H3K27 and H4K16 peptides (Figs. 4a,b lane 10 versus 9).

To further investigate the cooperativity between eRNAs and acetylated histones, we examined eRNA-dependent enhanced binding of BRD4 to histone octamers that were either unacetylated or acetylated by the histone acetyltransferase p300. As predicted, p300 efficiently acetylated the histone octamers as demonstrated by the increased acetylation of H3K27 and H3K9 (Fig. 4c, lanes 3, 4 and 7, 8). In comparison, no acetylation was detected in the absence of p300 or acetyl-CoA (Fig. 4c, lanes 1, 2 and 5, 6). The acetylated histone octamers were coupled to magnetic beads using H3K27ac and H3K9ac antibodies and then incubated with BRD4 in the presence or absence of *MMP9* eRNA. Notably and consistent with the histone peptide binding assay results, we found that *MMP9* eRNA significantly increased BRD4 binding to acetylated histone octamers (Fig. 4c, lane 4 versus 3). Also consistent, the *MMP9* eRNA had no effect on the binding of BRD4 ΔBD1/2 to the acetylated histone octamers (Fig. 4c, lanes 7 and 8 versus 5 and 6). The enhanced binding of BRD4 to

acetylated histone peptides and octamers in the presence of the *MMP9* eRNA (Figs. 4a-c) was further confirmed in the presence of the *CCL2* eRNA (Supplementary Figs. 3a,b). Moreover, by performing an eRNA titration experiment, we identified that several concentrations of the *MMP9* eRNA revealed enhanced BRD4 binding to acetylated histone octamers (Supplementary Fig. 3c, lanes 3 and 4 versus 2). In addition, at high molar ratios of *MMP9* eRNA to BRD4, the *MMP9* eRNA was found to inhibit BRD4 binding to the acetylated histone octamers (Supplementary Fig. 3c, lanes 6 and 7 versus 2). Taken together, these findings establish that BRD4-RNA interactions enhance BRD4 binding to acetylated histone substrates in an RNA concentration-dependent manner.

To gain insight into the steady state binding of BRD4 to acetylated histone H3 in the presence or absence of eRNAs, surface plasmon resonance (SPR) analyses were performed. Biotin-labeled H3K27ac-modified peptides were immobilized on a streptavidin-coated sensor chip surface and BRD4 BD1/2 was flowed over the chip surface at various concentrations (10, 15, 20 nM) in the presence or absence of *MMP9* eRNA. Notably and as demonstrated by the resulting sensorgrams (Fig. 4d), the amount of BRD4 BD1/2 that bound to the H3K27ac-modified peptides for all BRD4 protein concentrations was enhanced in the presence of *MMP9* eRNA to yield an absolute level of binding approximately threefold higher than observed in the absence of eRNA. An appreciable dissociation was not detected as the targeted BRD4 BD1/2 remained bound to the H3K27ac-modified peptide during the time course of the experiments (Fig. 4d). Notably, the sensorgrams also demonstrated that all concentrations of BRD4 BD1/2 reached a significantly higher maximum binding capacity (R_{max}) in the presence versus absence of eRNA (Fig. 4e). Specifically, the R_{max} of BRD4 to the H3K27ac-modified peptide increased linearly in the presence of eRNA (Fig. 4e). Whereas BRD4 BD1/2 binding to the acetylated H3 peptide was saturated in the absence of eRNA (Fig. 4e). Notably, these biophysical data together with our biochemical findings

indicate that eRNA interactions with BRD4 BDs play a pivotal role in the enhanced binding of BRD4 to acetylated histones, *in vitro.*

eRNAs regulate gene activation by modulating BRD4 enhancer occupancy and regulation of eRNA synthesis.

To investigate the biological significance of BRD4-eRNA interactions, we first employed shRNA-mediated knockdown of eRNAs in SW480 cells (+/- TNF-α). qRT-PCR analysis revealed that relative to a nontargeting control, shRNA oligonucleotides that target the *MMP9* (*MMP9* eRNA-1) and *CCL2* (*CCL2* eRNA-1) eRNAs revealed a significant and specific decrease in the TNF-α-induced levels of *MMP9* and *CCL2* eRNAs by approximately three-fold and six-fold, respectively (Fig. 5a). Notably, this decrease in *MMP9* and *CCL2* eRNA levels resulted in a significant (~three-fold) decrease in the *MMP9* and *CCL2* mRNA expression levels, respectively, thereby revealing a direct role for these TNF-α-induced eRNAs in the induction of proinflammatory gene expression (Fig. 5a). This reduction in the TNF-α-induced mRNA levels of *MMP9* and *CCL2* was further confirmed with a second shRNA oligonucleotide targeting different regions of the *MMP9* (*MMP9* eRNA-2) and *CCL2* eRNAs (*CCL2* eRNA-2) (Supplementary Fig. 4a). In addition, and consistent with the specificity of the eRNA knockdown effects, shRNA-mediated knockdown of the *MMP9* and *CCL2* eRNAs did not affect the eRNA and mRNA expression levels of *CCL2* and *MMP9*, respectively (Fig. 5a and Supplementary Fig. 4a) or that of *CPA4* and *CYP24A1* that are also significantly induced following TNF-α treatment (Supplementary Fig. 4b). Also, the gene-selective effects of the *MMP9* and *CCL2* eRNAs are not due to altered mutp53 or BRD4 protein levels, which were found to be unaffected by immunoblot analysis of whole cell lysates prepared from the eRNA knockdown cell lines (Fig. 5b). These results demonstrate the importance of the *MMP9* and *CCL2* eRNAs in regulating TNF-α-induced gene expression.

Having established significant knockdown of the *MMP9* and *CCL2* eRNAs, we next performed ChIP-qPCR in TNF-α-treated *MMP9* and *CCL2* eRNA knockdown cells to examine a direct role for these eRNAs in the regulation of BRD4 enhancer occupancy. Notably, BRD4 binding in the *MMP9* and *CCL2* eRNA-depleted cells was significantly and comparably (46% and 49%) reduced at the *MMP9* and *CCL2* enhancer regions, respectively (Fig. 5c). Notably, and consistent with the specificity of eRNA function, *MMP9* eRNA knockdown did not affect BRD4 binding at the *CCL2* enhancer region and vice versa (Fig. 5c). This significant loss of BRD4 binding upon eRNA knockdown resulted in a significant and comparable (54% and 66%) decrease in RNAPII binding at the *MMP9* and *CCL2* enhancers, respectively (Fig. 5c), which is consistent with the previously described roles of BRD4 in supporting RNAPII binding and elongation[34,35]. Moreover, we also tested the role of RNAs in the regulation of BRD4 enhancer binding by treating SW480 cells with Actinomycin D (Act D) that inhibits transcription, but does not affect BRD4 protein levels (Supplementary Fig. 4c). The significant decrease in the TNF-α-induced *MMP9* and *CCL2* eRNA expression levels following Act D treatment (Supplementary Fig. 4d) was accompanied by a significant decrease in TNF-α-induced BRD4 binding by 61% and 77%, at the *MMP9* and *CCL2* enhancers, respectively (Supplementary Fig. 4e). These findings together with our eRNA knockdown analyses demonstrate a role for RNAs in regulating BRD4 enhancer recruitment in response to TNF-α signaling.

Having demonstrated that eRNAs facilitate enhanced BRD4 binding to acetylated histones *in vitro* and at active enhancers with high levels of H3K27ac accumulation, we next investigated the effects of eRNAs on BRD4-dependent regulation of TNF-α-inducible eRNA and mRNA expression levels. ShRNA-resistant constructs expressing BRD4 FL or BRD4 ΔBD1/2 were transiently expressed in SW480 cells cotransduced with lentiviral shRNA specific for *MMP9* or *CCL2* eRNA and BRD4. Relative to the vector control, both BRD4 FL

and BRD4 ΔBD1/2 equivalently reconstituted BRD4 mRNA and protein levels in BRD4 knockdown cells (Fig. 5d). As expected, BRD4 FL, but not BRD4 ΔBD1/2 was able to fully rescue TNF-α-inducible *MMP9* and *CCL2* eRNA and mRNA expression levels in the BRD4 single knockdown cells (Fig. 5e). Notably however, the ability of BRD4 FL to rescue *CCL2* eRNA and mRNA expression levels in the double *CCL2* eRNA and BRD4 knockdown cell lines was significantly (2 to 3-fold) less efficient. Moreover, we observed that BRD4 FL was comparably (2- to 3-fold) less efficient in rescuing *MMP9* eRNA and mRNA levels in the BRD4 and *MMP9* knockdown cells (Fig. 5e). In addition, BRD4 ΔBD1/2 was unable to rescue the reduced expression of *MMP9* and *CCL2* eRNA and mRNA levels in the *MMP9 and CCL2* eRNA/BRD4 double knockdown cells, respectively (Fig. 5e). These rescue experiments confirm the specificity of our BRD4 knockdown experiments and, taken together with our *in vitro* analyses, demonstrate that eRNAs play a pivotal role in regulating BRD4 enhancer binding that is required to support BRD4-dependent regulation of enhancer transcription and gene activation in response to chronic TNF-α signaling.

Discussion

BRD4 regulates a class of mutp53 enhancers and target genes in response to chronic immune signaling

Enhancers are regulatory hubs that are selectively recognized by an array of transcription factors and co-activators that coordinate enhancer regulation of gene expression[1,2]. BRD4 is a well-known transcriptional coactivator that localizes at enhancers, especially clusters of enhancers (super enhancers) to regulate the transcription of the oncogenes, *MYC* and *BCL2*, which have important implications in human diseases that include, but are not limited to leukemia, multiple myeloma, and Burkitt lymphoma[19-21,52,53]. Our studies advance our understanding of BRD4's role in human cancer through the identification of the genome-wide binding of this coactivator at enhancers that are co-occupied by the potent oncogene

mutp53 that is known to drive aberrant gene expression in more than 50% of all human cancers. Notably, among the enhancers co-bound by mutp53 and BRD4 are several enhancers that have recently been shown to be regulated by mutp53 and NFκB and are linked to the potent activation of a proinflammatory gene expression program that leads to increased colon cancer cell growth and invasion potential[48]. In support of a functional relationship between mutp53 and BRD4, we found that purified BRD4 forms both direct interactions and physiological associations with mutp53 and is simultaneously bound with mutp53 at active enhancers in response to chronic TNF-α signaling. Furthermore, we demonstrated that mutp53 contributes to the recruitment of BRD4 at a subset of enhancers following chronic immune signaling. Our data also support the a role for BRD4 in regulating the activation of mutp53 and BRD4 co-bound enhancers as demonstrated by the significant decrease in TNF-α-induced eRNA levels following BRD4 shRNA-mediated knockdown or inhibition by JQ1 and the significantly higher eRNA levels found at BRD4 and mutp53 co-bound enhancers versus enhancers that are devoid of both BRD4 and mutp53. These findings that support a role for BRD4 in promoting the activation of mutp53 target genes by modulating enhancer activation in response to chronic immune signaling underscore the significance for mutp53 and BRD4 cooperativity in colon cancer cells. Our findings reported here and future studies testing the roles of BRD4 in regulating mutp53-dependent gene expression programs are also likely to have clinical significance given the widespread roles of mutp53 and BRD4 in cancer and due to the potential for pharmacological inhibition of BRD4 through the targeting of small molecules including JQ1.

eRNAs interact with BRD4 to affect transcriptional activation

Given the prevalence of eRNAs in various cell types and in response to stimuli[39-41,48,54-60], a number of functions for eRNAs in transcription can be envisioned. For example, it has been demonstrated that eRNAs interact directly with the transcriptional coactivator, Mediator[41,43].

In addition, eRNAs function by promoting the chromatin modifying activities of the histone acetyltransferase CBP[44] and by promoting chromatin accessibility through currently unknown mechanisms[41]. One possibility for how eRNAs could affect chromatin accessibility at enhancers may include direct effects on the SWI/SNF chromatin remodeler subunits BRG1 and BRD7, which is supported by our finding that the BDs of BRG1 and BRD7 directly interact with eRNAs in this study. Overall, our results provide strong evidence for the functional significance of eRNAs in stimulating transcription by enhancing BRD4 binding to acetylated histones. Specifically, we demonstrate that eRNAs form physiological associations and direct interactions with the tandem bromodomains of BRD4, which in turn promotes enhanced BRD4 binding to acetylated forms of both histone H3 and H4 peptides as well as acetylated histone octamers. Our biochemical and biophysical findings are corroborated by our cell-based findings that show the importance of eRNAs in regulating the enhancer binding of BRD4. Strikingly, the depletion of TNF-α-inducible eRNA levels results in a significant decrease in the enhancer binding of BRD4, which in turn leads to a significant loss of RNAPII occupancy and a significant decrease in inflammation-induced gene expression in human colon cancer cells. Our studies also underscore the significance of BRD4-eRNA interactions in regulating enhancer-dependent gene activation by revealing the recovery of eRNA and tumor promoting gene expression by shRNA resistant BRD4 FL, but not BRD4 ΔBD in BRD4 single knockdown but not BRD4 and eRNA double knockdown cells. Taken together, our studies reported here, support a model (Fig. 6) for a positive feedback loop in which eRNAs could be involved in the *cis* recruitment of BRD4 at mutp53 bound enhancers for augmented enhancer and gene activation. Furthermore, this model supports the functional interplay between histone modifications and eRNAs, which emphasizes that eRNAs are not required for the initial recruitment of BRD4 but rather cooperatively impact its binding potential after BRD4 has bound to acetylated histones. This

cooperativity between epigenetic mechanisms as revealed by our data showing that the acetyl-lysine recognition BDs interact with eRNAs together with previous studies showing that the methyl-lysine recognition chromodomain of CBX7CD binds lncRNA *ANRIL*[61], suggest that eRNAs, similar to lncRNAs are likely to function through chromatin effector domains to impact chromatin and gene regulation. Importantly, our studies did not rule out whether other known BRD4 functional activities including its atypical histone modifying activity[62] are affected by eRNAs.

We demonstrate that BRD4 binds a broad spectrum of RNA transcripts, which suggests its promiscuous relationship with RNAs. Although RNA sequence does not appear to contribute to the specificity of BRD4-RNA interactions, and while we cannot rule out structural contributions of RNA from our analyses, we have found that BRD4 forms associations with RNAs in an enhancer/locus-specific manner. These results are supported by our BRD4 UV-RIP, BRD4 ChIP-seq, and GRO-seq analyses that together demonstrate the identification that BRD4 forms associations with RNAs that are produced specifically from genomic regions that are also highly occupied by BRD4 following chronic TNF-α signaling. This observation is consistent with a recent study showing that CBP also associates with RNAs that are produced at genomic regions where there exists high levels of CBP bound[44]. Our findings further demonstrate that shRNA-resistant BRD4 FL was able to reconstitute the expression levels of specific eRNAs in BRD4-depleted cells but not in BRD4 and eRNA-double knockdown cells. Specifically, we show that the ability of BRD4 to reconstitute *MMP9* and *CCL2* eRNA levels occurs in the *CCL2* and *MMP9,* but not the *MMP9* and *CCL2* eRNA double knockdown cells, respectively, which is further consistent with enhancer/locus-specific eRNA-BRD4 associations.

eRNAs interact with the highly conserved acetyl-lysine recognition bromodomain

Our identification of this unexpected mechanism of eRNA function in regulating the chromatin binding and transcriptional coactivator functions of BRD4 could be widespread given that BDs are evolutionarily conserved protein interacting modules[12] and were mapped in this study as the eRNA-interacting domains of BRD4. In support of the generality of this finding, we identified that the tandem BDs of all BET family members that include BRD2, BRD3, BRD4, and BRDT, and the single BD-containing, non-BET proteins, BRG1 and BRD7 form interactions with eRNAs. These results further demonstrated that while the RNA associations of the BRG1 and BRDT BDs are significantly above background, they are weaker relative to the BD-RNA interactions of BRD2, BRD3, BRD4, and BRD7. This variable level of RNA binding to various BDs is consistent with known differences in BD structure and conformation, which have been linked to disparities in the interactions of various BDs with acetylated residues in histones and other proteins and diverse roles in regulating transcription[63]. Moreover, given the development of inhibitors that are specific to the BDs of various members of the BET family and that have shown promising results in regulating gene expression in disease, particularly in cancer[64], eRNAs that bind to BDs could be potent therapeutic targets to repress pro-tumorigenic gene expression programs.

Our observation that eRNAs through BD interactions enhance BRD4 binding to acetylated histones and octamers suggest that eRNAs are likely to interact with the BD in a region that is independent of the acetyl lysine-recognition domain. While BDs are categorized into eight distinct classes based on their diverse structures, they share four conserved α-helices that are connected to one another by loops of variable lengths[15,63]. Conserved amino acids located within these loops facilitate the docking of acetylated lysine residues and the surface that surrounds the acetyl binding pocket is often comprised of a patch of basic amino acids that have been shown to further prompt interactions with the backbone of acetylated substrates[11,63]. It is possible that this positively charged surface found

in BDs could also facilitate interactions with negatively charged nucleic acids, including eRNAs. This possibility is consistent with recent studies that have shown that this positively charged patch facilitates interactions of the BRDT BD1[65] and more recently the BRG1/hBRM BDs[66] with DNA that in turn, facilitate acetylation-dependent nucleosome binding of these BD-containing proteins[65,66]. Furthermore, point mutations in the positively charged patch within the hBRM BD were found to significantly reduce hBRM's binding to DNA, while not disrupting BD interactions with H3K14 acetylated peptides[66]. This finding suggests that BD interactions with nucleic acids are likely to occur outside the region that is required for acetyl-lysine recognition and thereby could allow for RNA/DNA interactions that enhance BD association with acetyl-lysines. In addition, differences in the number of basic amino acids within the BD loops could contribute to variations in the electrostatic charge that together with variable structural/conformational contributions and other potential regulatory mechanisms, may predict the variable levels of interaction that we observed between eRNAs and different BDs assessed in our study. Furthermore, these variations could also explain the differences in BD interactions with DNA versus that of RNA. Specifically, the analyses of BRD4 interactions with DNA revealed that DNA associations occur only with the BRD4 BD2 and not BD1[65]. In comparison, we found that BRD4 BD1 and BD2 interact with eRNAs weakly and that the tandem BDs of BRD4 are required to support eRNA interactions that are comparable to the naturally occurring, shorter isoform of BRD4 (BRD4 1-722). Future studies are needed to determine the functional importance of BD contacts with DNA versus RNA and the differential regulatory mechanisms that govern these BD interactions.

Our demonstration that each of the tandem BRD4 BDs (BD1 and BD2) are required to reconstitute BRD4 interactions with eRNAs, together with our data demonstrating the significance of bivalent interactions of BDs with acetylated lysines and eRNAs is consistent

with previous reports revealing the importance of multivalency in chromatin regulation. Specifically, the overall affinity and specificity of chromatin binding can be significantly enhanced by multiple chromatin interacting domains within a single chromatin reader or through the multiple chromatin interacting proteins that are often present in multiprotein complexes[67]. Consistent, is the identification that the BDs of the BET family exhibit modest affinity for monoacetylated lysine, however the affinity of their binding is significantly increased when the BDs are anchored to multiple acetylation sites[11,14,51]. Future studies are needed to extend the implications of BD-RNA interactions and test how BDs engage these epigenetic modifiers to transduce downstream function.

Taken together, our findings are consistent with the emerging notion that eRNAs are functional molecules, rather than merely reflections of enhancer activation or simply transcriptional noise. Our studies provide mechanistic insights into the role of enhancer transcripts that directly interact with BRD4 at active enhancers, which leads to increased RNAPII binding, eRNA synthesis, and the transcription of proinflammatory genes. These findings provide a framework for understanding eRNAs and their convergence with histone modifications in the regulation of transcriptional coactivators.

METHODS

Cell culture and treatments Human colorectal adenocarcinoma SW480 cells and human embryonic kidney 293T (HEK293T) cells were purchased from American Type Culture Collection (ATCC) and grown in Dulbecco's modified Eagle medium (DMEM, Gibco) supplemented with 10% fetal bovine serum (FBS, Gibco). SW480 cells that stably and inducibly express short hairpins against LacZ or p53 were kindly provided by Xinbin Chen (UC Davis) and were grown in standard DMEM medium containing penicillin and streptomycin (Gemini Bio-Products), 1.5 μg ml^{-1} puromycin (Sigma), and were induced with 1 μg ml^{-1} doxycycline (Sigma). Lentivirus infected SW480 cells were propagated in growth

medium containing DMEM, 10% FBS, 100 units ml^{-1} penicillin, 100 μg ml^{-1} streptomycin, and 1.5 μg ml^{-1} puromycin. For experiments with TNF-α treatment, the indicated cells were treated with 12.5 ng ml^{-1} recombinant TNF-α (Shenandoah Biotechnology) for the indicated time points before harvesting for gene expression or ChIP analyses. SW480 cells were treated with a final concentration of 500 nM JQ1 (Cayman Chemical) or vehicle (DMSO, Fisher Scientific) before harvesting for gene expression and immunoblot analyses. All cell lines mentioned have tested negative for mycoplasma contamination by PCR.

Immunoblotting Protein samples were incubated at 95 °C for 5 min, separated by SDS-PAGE, and transferred to PVDF membranes (EMD Millipore) that were probed with the indicated antibodies. Reactive bands were detected by ECL (Thermo Scientific Pierce), and exposed to Blue Devil Lite ECL films (Genesee Scientific) or visualized by LI-COR (LI-COR Biosciences).

Antibodies Antibodies used for ChIP assays were obtained commercially as follows: anti-BRD4 (A301-985A100, 1 μg) from Bethyl laboratories; anti-RNAPII (N20, sc899, 1 μg), anti-IgG (sc2027, 1 μg) from Santa Cruz Biotechnology. Antibodies used for immunoblotting were obtained as follows: anti-BRD4 (1:3000 dilution) from Bethyl laboratories, anti-H3 (ab1791, 1:5000 dilution), anti-H3K27ac (ab4729, 1:5000 dilution) from Abcam; anti-H3K9ac (13-0020, 1:5000 dilution) from EpiCypher; and anti-p53 (DO1, sc126, 1:2000 dilution) and anti-β-Actin (sc47778, 1:2000 dilution) from Santa Cruz Biotechnology.

Lentivirus production and transduction pLKO.1 TRC control and target shRNA plasmids were generated with annealed primers to knockdown BRD4 and *MMP9* and *CCL2* eRNAs. shRNA primers used in this study are listed in Supplementary Table 1. For lentivirus production and transduction, 50-60% confluent HEK293T cells were transfected with Lipofectamine 3000 (Invitrogen) with TRC control, target shRNAs, and packaging plasmids psPAX2 and pMD2.G. Virus-containing medium was collected 48 and 72 hr post

transfection, filtered with a 0.45μm pore size filter, and used for viral infection. SW480 cells were transduced with the viral supernatants containing 8 μg ml^{-1} polybrene (Sigma-Aldrich). After 8 hr infection, virus-containing medium was removed and replaced with fresh medium. After 48 hr, puromycin was added to a final concentration of 1.5 μg ml^{-1}. Cells were cultured for an additional 72 hr before harvesting the cells for qRT-PCR and immunoblot to confirm successful knockdown efficiency.

***In vitro* RNA synthesis** Primers were designed to amplify desired genomic regions that correspond to maximal eRNA (GRO-seq) peaks at *MMP9* and *CCL2* enhancers and *MEG3* and *p21* exonic sequences. Primers sequences can be found in Supplementary Table 5. The T7 promoter sequence was included in the forward primer and genomic fragments were PCR amplified from HeLa genomic DNA (NEB), confirmed by sequencing, and subsequently used for RNA synthesis using T7 RiboMAX Express Large Scale RNA Production System (Promega). Synthesized RNAs were purified per manufacturer's instructions and quantitated by Nanodrop (Invitrogen). RNA probes were refolded by incubation at 95 ºC for 5 min followed by snap-cooling on ice for 5 min. Cold RNA refolding buffer (10 mM Tris-HCl at pH 7, 100 mM KCl, 10 mM $MgCl_2$) was then added and the samples were transferred to an ice-cold metal rack. RNAs were allowed to refold by warming the sample to room temperature for 20-30 min.

RNA purification and quantitative real-time PCR Total RNA was extracted with TRIzol LS reagent (Invitrogen) from SW480 stably expressing control, BRD4, or *CCL2* and *MMP9* eRNA shRNAs and treated with 12.5 ng ml^{-1} TNF-α for the indicated time points. Total RNA (0.5-1 μg) was used for cDNA synthesis using ProtoScript II First Strand cDNA Synthesis Kit (NEB) with random hexamers. PCR reactions were performed on an Applied Biosystems Step One Plus real-time PCR systems using SYBR Green PCR Master Mix (Applied Biosystems) in duplicate using samples from at least three independent cell harvests

and the specificity of amplification was examined by melting curve analysis. The relative levels of eRNA and mRNA expression were calculated according to the (ΔΔCt) method and individual expression data was normalized to *GAPDH*. The gene expression levels determined after TNF-α treatment are relative to the levels before TNF-α treatment. Primers for qRT-PCR are listed in Supplementary Table 2.

Ultraviolet-RNA Immunoprecipitation (UV-RIP) SW480 cells treated with TNF-α for 0 or 16 hr were crosslinked by UV irradiation (150 mJ per cm^2 at 254 nm) using a Stratalinker and lysed in RIP lysis buffer [25 mM HEPES-KOH at pH 7.5, 150 mM KCl, 0.5% NP40, 1.5 mM $MgCl_2$, 10% glycerol, 1 mM EDTA, 0.05% NP40, 0.4 U RNase inhibitor (Promega), protease inhibitor cocktails (PICs)] on ice for 30 min. Cleared cell lysates were used for IP with BRD4 and IgG-antibody bound Protein A Dynabeads (Invitrogen) overnight. Beads were subsequently washed three times with RIP lysis buffer and RNA samples were eluted using TRIzol LS reagent. cDNA samples were prepared as described above and analyzed by qRT-PCR primers listed in Supplementary Table 2.

Histone peptide binding assays Unmodified H3 (21-44), K27ac-modified H3 (21-44), unmodified H4 (1-25), or K16ac-modified H4 (1-25) peptides (Innopep Inc.) were immobilized on Dynabeads MyOne Streptavidin C1 (Life technologies) and subsequently incubated with 200 ng of recombinant FLAG-BRD4 FL or FLAG-BRD4 *Δ*BD1/2 in the absence or presence of 0.2 nM refolded *MMP9* or *CCL2* eRNA in binding buffer (150 mM NaCl, 20 mM HEPES-KOH at pH 7.9, 0.1% NP40, 0.25 mg ml^{-1} bovine serum albumin (BSA), 1 mM Sodium butyrate, 1mM PMSF, PICs, RNase inhibitor) for 4 hr at 4°C. Beads were washed ten times with binding buffer containing 400 mM NaCl. Bound proteins were eluted in sample buffer and analyzed by SDS-PAGE and immunoblotting.

Histone acetyltransferase (HAT) assays Recombinant histone octamers (0.5 μg) that were purified as previously described[68] were incubated with p300 (30 ng) and acetyl-CoA (20 μM)

in reaction buffer (50 mM HEPES pH 7.8, 30 mM KCl, 0.25 mM EDTA, 5.0 mM MgCl2, 5.0 mM sodium butyrate, 2.5 mM DTT). Reactions were incubated at 30˚C for 30 min, resolved by SDS-PAGE, and analyzed by immunoblotting.

Histone octamer binding assays p300-acetylated histone octamers were isolated by incubating the HAT reactions with H3K9ac and H3K27ac antibody-coupled Protein A Dynabeads in binding buffer (150 mM NaCl, 50 mM Tris-HCl at pH 8.0, 0.1% NP40, 1 mM Sodium butyrate, 1 mM PMSF, PICs) for 3 hr at 4 ºC. Following the incubation, the acetylated histone octamer bound beads were washed three times with binding buffer and then incubated with 200 ng of recombinant FLAG-BRD4 FL or FLAG-BRD4 ΔBD1/2 in the absence or presence of 0.2 nM refolded eRNA or increasing doses in the range of 0.06 nM to 2 nM in binding buffer with 1% BSA for 12 hr at 4 ºC. The protein complexes were washed eight times with wash buffer (400 mM NaCl, 50 mM Tris-HCl at pH 8.0, 0.1% NP40, 0.5% BSA, 1 mM Sodium butyrate, 1 mM PMSF, PICs). Bound proteins were eluted in sample buffer and analyzed by SDS-PAGE and immunoblotting with the indicated antibodies.

Surface plasmon resonance (SPR) assays Sensorgrams were recorded on a BIAcore 3000 instrument using streptavidin (SA) chips. Biotinylated H3K27ac histone peptide was immobilized on the SA chip in binding buffer (150 mM NaCl, 20 mM HEPES-KOH at pH 7.9, 0.1% NP40). Sensorgrams were run in the automatic subtraction mode using flow cell 1 (FC 1) as an unmodified reference. Data was collected for FC's 2, 3, and 4, which contained varying amounts of the BD1/2 domain of BRD4 and in the presence or absence of 0.2 nM refolded *MMP9* eRNA with 100 Response Units (RU) immobilized on FC2, 200 RU on FC3, and 400 RU on FC4. Injections were made using the kinject injection mode with a 3 min contact time and a 3 min dissociation phase, at a flow rate of 50 μl min^{-1}. The running buffer used for the binding experiments was 150 mM NaCl, 20 mM HEPES-KOH at pH 7.9, 0.1% NP40. The data was analyzed using the BIA Evaluation 4.1 software.

Co-immunoprecipitation Assays were performed using whole cell lysates prepared from SW480 cells that were treated with 12.5 ng ml^{-1} TNF-α for 0 or 16 hr. Cleared lysates were first incubated with indicated antibodies for 2 hr at 4 ºC followed by an additional 2 hr incubation with Protein A Sepharose (Rockland Inc.). Beads were washed with wash buffer (20 mM Tris-HCl at pH 7.9, 0.1% NP40, 150 mM KCl) five times and analyzed by immunoblotting.

Chromatin Immunoprecipitation (ChIP) and ChIP-Seq BRD4 ChIP assays were performed using SW480 cells that were (i) untreated or treated with 12.5 ng ml^{-1} TNF-α for the indicated time points or (ii) transduced with indicated shRNAs and treated with 12.5 ng ml^{-1} TNF-α for 0 or 16 hr. Cells were sequentially cross-linked using 6 mM DSG (disuccinimidyl glutarate; ProteoChem) for 30 min and a final concentration of 1% formaldehyde for 10 min at room temperature and stopped with 125 mM glycine (Fisher Scientific). Cells were lysed in lysis buffer (20 mM Tris-HCl at pH 7.5, 300 mM NaCl, 2 mM EDTA, 0.5% NP40, 1% Triton X-100, 1 mM PMSF, PICs) and incubated on ice for 30 min. The resuspended cells were then dounced in an ice-cold homogenizer. Nuclear pellets were collected and resuspended in shearing buffer (0.1% SDS, 0.5% N-lauroylsarcosine, 1% Triton X-100, 10 mM Tris-HCl at pH 8.1, 100 mM NaCl, 1 mM EDTA, 1 mM PMSF, PICs). Isolated chromatin was fragmented to an average size of 200-600 bp with a bioruptor Pico (Diagenode). Precleared chromatin was immunoprecipitated overnight at 4 ºC and immunocomplexes were collected with protein A Dynabeads. The immunocomplexes were washed eight times in wash buffer (50 mM HEPES-KOH at pH 7.6, 500 mM LiCl, 1 mM EDTA, 1% NP40, 0.7% sodium deoxycholate, 1 mM PMSF, PICs), followed by two 1X TE washes, and eluted in elution buffer (50 mM Tris-HCl at pH 8.0, 10 mM EDTA, 1% SDS), crosslinks were reversed at 65 ºC for 4 hr or overnight, and DNA was purified using DNA Clean & Concentrator Kit according to the manufacturer's instructions. PCR reactions were

performed on an Applied Biosystems Step One Plus real-time PCR systems using SYBR Green PCR Master Mix in duplicate using samples from at least three independent cell harvests and the specificity of amplification was examined by melting curve analysis. The relative amounts of ChIP DNA were quantified relative to inputs. Primers for ChIP-quantitative PCR are listed in Supplementary Table 3. Sequential ChIP experiments were performed exactly as described above with minor modifications. Specifically, 150 μg of sheared chromatin was used to perform the IP. Following the washes after the first IP, immunocomplexes were eluted in re-IP elution buffer (50 mM Tris-HCl at pH 8.0, 1% SDS, 1 mM EDTA, 1 mM DTT, 1 mM PMSF, PICs) and diluted 10 fold in dilution buffer (16.7 mM Tris-HCl at pH 8.0, 167 mM NaCl, 0.01% SDS, 1% Triton X-100, 1.2 mM EDTA, 1 mM PMSF, PICs). The second IP was performed with indicated antibodies overnight at 4 ºC, followed by additional washes and the final elution as described above.

For ChIP-seq experiments, the IP's were performed as described. The eluted ChIP DNA was quantified using a Qubit 2.0 fluorometer (Invitrogen), and 2-5 ng of ChIP DNA was used to prepare the sequencing libraries from two biological replicates using the TruSeq ChIP Sample Prep Kit according to the manufacturer's instructions (Illumina). Briefly, ChIP DNA was end-repaired and adaptors were ligated to the ends of the DNA fragments. Adaptor-ligated ChIP DNA fragments with average size of 350 bp were used to construct libraries and single-end sequenced (50 bp) on Illumina HiSeq 4000. Sequencing reads were mapped to the hg38 human genome using Bowtie2 software 38 and default parameters. The mapped reads were then processed to make Tag Directory module using HOMER for filtering. Briefly, PCR duplications were removed and only uniquely mapped reads were kept for further analysis. The genome browser files for the resulting reads were generated by using make UCSC file module from HOMER. Enriched regions for BRD4 were called using find Peaks module from HOMER by using preset options, factor or histone styles respectively and

compared to the corresponding inputs. Deeptools were used to generate heat maps. *De novo* motif analysis was performed using the BRD4/mutp53 co-bound enhancer regions using "findMotifsGenome.pl" of Homer with ±100 bp window relative to the peak center.

Purification of recombinant proteins Mutant p53 R273H was generated by site-directed mutagenesis (Agilent Technologies). FLAG-BRD4 BD1/2, BD1, BD2 were cloned into pET11d bacteria expression vector using *Nde*I and *BamH*I sites after amplification from BRD4 cDNA. His-tagged tandem BDs (BD1/2) of BRD2, BRD3, BRD4, and BRDT as well as the single BDs of BRG1 and BRD7 were cloned into pET 6His bacteria expression vector using *BamHI* and *EcoRI* sites. p53 and BD constructs were expressed in *E. Coli* and purified on FLAG M2 agarose beads (Sigma) or TALON metal affinity resin (Clontech). The FLAG BRD4 FL and ΔBD1/2 proteins were expressed in Sf9 cells and purified on FLAG M2 agarose. Primers used for cloning are listed in Supplementary Table 4.

***In vitro* pull-down RNA binding assays** FLAG- and His-tagged proteins were incubated with 500 ng of refolded RNA while rotating at 4 ºC for 1 hr in RNA Binding Buffer (20 mM Tris-HCl at pH 7.4, 100 mM KCl, 0.2 mM EDTA, 0.05% NP40, 0.4 U RNase inhibitor, PICs). Protein-RNA complexes were recovered using FLAG M2 agarose beads or TALON resin for 1 hr at 4 ºC. Beads were washed three times with RNA wash buffer (20 mM Tris-HCl at pH 7.4, 200 mM KCl, 0.2 mM EDTA, 0.05% NP40, 0.4 U RNase inhibitor, PICs) and RNA samples were eluted using Trizol LS reagent. Purified RNA samples were resolved on a denaturing 5% TBE urea gel and stained with SYBR gold for 30 min before imaging using a Typhoon phosphorimager or LI-COR (LI-COR Biosciences).

RNA electrophoretic mobility shift assay (EMSA) EMSAs were performed following established protocols[69]. Binding reactions were performed in 1x RNA EMSA buffer (20 mM Tris-HCl at pH 7.4, 100 mM KCl, 1 mM EDTA, 1% glycerol, 0.05% NP40, 0.5 mM $ZnCl_2$, 0.1 mg ml^{-1} BSA (Fisher), 0.1 mg ml^{-1} yeast tRNA (Sigma), 2 mM DTT, 0.4 U RNase

inhibitor). The binding reactions were initiated by adding different doses (0.3-1.5 μg) of FLAG-BRD4 protein in the presence of 12,000 cpm refolded RNA and allowed to proceed for 30 min at 4 ºC. Reactions were loaded immediately on 6% Native polyacrylamide gels that was pre-run for 1 hr at 100V in 0.5X TBE at 4 ºC. The gel was run for 4 hr at 100V and exposed to autoradiography screen before imaging with Typhoon phosphorimager. For competition assays, (0, 50, 150, or 450 nM) of unlabeled RNA or ssDNA was added in addition to the ^{32}P radiolabeled RNA.

Data availability All sequencing data that support the findings of this study will be deposited in the National Center for Biotechnology Information Gene Expression Omnibus (GEO) and will be accessible through the GEO Series upon acceptance. All other relevant data are available from the corresponding author upon reasonable request.

Acknowledgements

We are grateful to Cheng-Ming Chiang (UT Southwestern) for providing the pF:hBRD4 (1-722)-11d, pcDNA3-F:hBRD4 FL, pcDNA3-F:hBRD4 ΔBD1/2 plasmids and BRD4 FL and BRD4 ΔBD1/2 expressing baculovirus. We are also thankful to Xinbin Chen (UC Davis) for providing the SW480 shLacZ and shp53 cell lines. H.R. was supported by the UCSD Cellular and Molecular Genetics Training Program through an institutional grant from the National Institute of General Medicine (T32 GM007240). This work was supported by the Research Scholar Award from the Sidney Kimmel Foundation for Cancer Research #857A6A to S.M.L., American Cancer Society ACS-IRG #70-002 to S.M.L, and University of California Cancer Research Coordinating Committee, CRN-17-420616 to S.M.L.

Author contributions

Conceptualization, H.R., J.L., Z. S., and S.M.L.; Methodology, H.R., J.L., Z.S., H.L., K.M.R., E.A.K, and S.M.L.; Investigation, H.R., J.L., Z.S., H.L., K.M.R., and S.M.L.; Formal Analysis, H.R., J.L., H.L., Z.S., E.A.K., and S.M.L.; Writing - Original Draft, H.R.,

J.L., and S.M.L.; Writing - Review & Editing, H.R., J.L., E.A.K, and S.M.L.; Funding Acquisition, S.M.L.; Supervision, S.M.L.

Conflict of interest

The authors declare no conflict of interest.

References

1. Calo, E. & Wysocka, J. Modification of enhancer chromatin: what, how, and why? *Mol Cell* **49**, 825-37 (2013).
2. Heinz, S., Romanoski, C.E., Benner, C. & Glass, C.K. The selection and function of cell type-specific enhancers. *Nat Rev Mol Cell Biol* **16**, 144-54 (2015).
3. Heintzman, N.D. et al. Histone modifications at human enhancers reflect global cell-type-specific gene expression. *Nature* **459**, 108-12 (2009).
4. Thurman, R.E. et al. The accessible chromatin landscape of the human genome. *Nature* **489**, 75-82 (2012).
5. Visel, A. et al. ChIP-seq accurately predicts tissue-specific activity of enhancers. *Nature* **457**, 854-8 (2009).
6. Chepelev, I., Wei, G., Wangsa, D., Tang, Q. & Zhao, K. Characterization of genome-wide enhancer-promoter interactions reveals co-expression of interacting genes and modes of higher order chromatin organization. *Cell Res* **22**, 490-503 (2012).
7. Creyghton, M.P. et al. Histone H3K27ac separates active from poised enhancers and predicts developmental state. *Proc Natl Acad Sci U S A* **107**, 21931-6 (2010).
8. Rada-Iglesias, A. et al. A unique chromatin signature uncovers early developmental enhancers in humans. *Nature* **470**, 279-83 (2011).
9. Wang, D. et al. Reprogramming transcription by distinct classes of enhancers functionally defined by eRNA. *Nature* **474**, 390-4 (2011).
10. Marushige, K. Activation of chromatin by acetylation of histone side chains. *Proc Natl Acad Sci U S A* **73**, 3937-41 (1976).
11. Filippakopoulos, P. & Knapp, S. The bromodomain interaction module. *FEBS Lett* **586**, 2692-704 (2012).
12. Filippakopoulos, P. et al. Histone recognition and large-scale structural analysis of the human bromodomain family. *Cell* **149**, 214-31 (2012).
13. Umehara, T. et al. Structural basis for acetylated histone H4 recognition by the human BRD2 bromodomain. *J Biol Chem* **285**, 7610-8 (2010).
14. Moriniere, J. et al. Cooperative binding of two acetylation marks on a histone tail by a single bromodomain. *Nature* **461**, 664-8 (2009).
15. Dhalluin, C. et al. Structure and ligand of a histone acetyltransferase bromodomain. *Nature* **399**, 491-6 (1999).
16. Mujtaba, S., Zeng, L. & Zhou, M.M. Structure and acetyl-lysine recognition of the bromodomain. *Oncogene* **26**, 5521-7 (2007).
17. Yang, X.J. Lysine acetylation and the bromodomain: a new partnership for signaling. *Bioessays* **26**, 1076-87 (2004).
18. Zeng, L. & Zhou, M.M. Bromodomain: an acetyl-lysine binding domain. *FEBS Lett* **513**, 124-8 (2002).
19. Dawson, M.A. et al. Inhibition of BET recruitment to chromatin as an effective treatment for MLL-fusion leukaemia. *Nature* **478**, 529-33 (2011).

20. Delmore, J.E. et al. BET bromodomain inhibition as a therapeutic strategy to target c-Myc. *Cell* **146**, 904-17 (2011).
21. Zuber, J. et al. RNAi screen identifies Brd4 as a therapeutic target in acute myeloid leukaemia. *Nature* **478**, 524-8 (2011).
22. Huang, B., Yang, X.D., Zhou, M.M., Ozato, K. & Chen, L.F. Brd4 coactivates transcriptional activation of NF-kappaB via specific binding to acetylated RelA. *Mol Cell Biol* **29**, 1375-87 (2009).
23. Zou, Z. et al. Brd4 maintains constitutively active NF-kappaB in cancer cells by binding to acetylated RelA. *Oncogene* **33**, 2395-404 (2014).
24. Wu, S.Y., Lee, A.Y., Lai, H.T., Zhang, H. & Chiang, C.M. Phospho switch triggers Brd4 chromatin binding and activator recruitment for gene-specific targeting. *Mol Cell* **49**, 843-57 (2013).
25. Brown, J.D. et al. NF-kappaB directs dynamic super enhancer formation in inflammation and atherogenesis. *Mol Cell* **56**, 219-231 (2014).
26. Roe, J.S., Mercan, F., Rivera, K., Pappin, D.J. & Vakoc, C.R. BET Bromodomain Inhibition Suppresses the Function of Hematopoietic Transcription Factors in Acute Myeloid Leukemia. *Mol Cell* **58**, 1028-39 (2015).
27. Shi, J. et al. Disrupting the interaction of BRD4 with diacetylated Twist suppresses tumorigenesis in basal-like breast cancer. *Cancer Cell* **25**, 210-25 (2014).
28. Stewart, H.J., Horne, G.A., Bastow, S. & Chevassut, T.J. BRD4 associates with p53 in DNMT3A-mutated leukemia cells and is implicated in apoptosis by the bromodomain inhibitor JQ1. *Cancer Med* **2**, 826-35 (2013).
29. Lee, J.E. et al. Brd4 binds to active enhancers to control cell identity gene induction in adipogenesis and myogenesis. *Nat Commun* **8**, 2217 (2017).
30. Loven, J. et al. Selective inhibition of tumor oncogenes by disruption of super-enhancers. *Cell* **153**, 320-34 (2013).
31. Brown, J.D. et al. NF-kappaB directs dynamic super enhancer formation in inflammation and atherogenesis. *Mol Cell* **56**, 219-31 (2014).
32. Hah, N. et al. Inflammation-sensitive super enhancers form domains of coordinately regulated enhancer RNAs. *Proc Natl Acad Sci U S A* **112**, E297-302 (2015).
33. Chen, J. et al. BET Inhibition Attenuates Helicobacter pylori-Induced Inflammatory Response by Suppressing Inflammatory Gene Transcription and Enhancer Activation. *J Immunol* **196**, 4132-42 (2016).
34. Jang, M.K. et al. The bromodomain protein Brd4 is a positive regulatory component of P-TEFb and stimulates RNA polymerase II-dependent transcription. *Mol Cell* **19**, 523-34 (2005).
35. Winter, G.E. et al. BET Bromodomain Proteins Function as Master Transcription Elongation Factors Independent of CDK9 Recruitment. *Mol Cell* **67**, 5-18 e19 (2017).
36. Kanno, T. et al. BRD4 assists elongation of both coding and enhancer RNAs by interacting with acetylated histones. *Nat Struct Mol Biol* **21**, 1047-57 (2014).
37. Li, W., Notani, D. & Rosenfeld, M.G. Enhancers as non-coding RNA transcription units: recent insights and future perspectives. *Nat Rev Genet* **17**, 207-23 (2016).
38. Kim, T.K. & Shiekhattar, R. Architectural and Functional Commonalities between Enhancers and Promoters. *Cell* **162**, 948-59 (2015).
39. Hsieh, C.L. et al. Enhancer RNAs participate in androgen receptor-driven looping that selectively enhances gene activation. *Proc Natl Acad Sci U S A* **111**, 7319-24 (2014).
40. Li, W. et al. Functional roles of enhancer RNAs for oestrogen-dependent transcriptional activation. *Nature* **498**, 516-20 (2013).
41. Mousavi, K. et al. eRNAs promote transcription by establishing chromatin accessibility at defined genomic loci. *Mol Cell* **51**, 606-17 (2013).

42. Schaukowitch, K. et al. Enhancer RNA facilitates NELF release from immediate early genes. *Mol Cell* **56**, 29-42 (2014).
43. Maruyama, A., Mimura, J. & Itoh, K. Non-coding RNA derived from the region adjacent to the human HO-1 E2 enhancer selectively regulates HO-1 gene induction by modulating Pol II binding. *Nucleic Acids Res* **42**, 13599-614 (2014).
44. Bose, D.A. et al. RNA Binding to CBP Stimulates Histone Acetylation and Transcription. *Cell* **168**, 135-149 e22 (2017).
45. Liu, W. et al. Brd4 and JMJD6-associated anti-pause enhancers in regulation of transcriptional pause release. *Cell* **155**, 1581-1595 (2013).
46. Zhang, W. et al. Bromodomain-containing protein 4 (BRD4) regulates RNA polymerase II serine 2 phosphorylation in human CD4+ T cells. *J Biol Chem* **287**, 43137-55 (2012).
47. Sengupta, D. et al. Disruption of BRD4 at H3K27Ac-enriched enhancer region correlates with decreased c-Myc expression in Merkel cell carcinoma. *Epigenetics* **10**, 460-6 (2015).
48. Rahnamoun, H. et al. Mutant p53 shapes the enhancer landscape of cancer cells in response to chronic immune signaling. *Nat Commun* **8**, 754 (2017).
49. Wu, S.Y. & Chiang, C.M. The double bromodomain-containing chromatin adaptor Brd4 and transcriptional regulation. *J Biol Chem* **282**, 13141-5 (2007).
50. Chiang, C.M. Brd4 engagement from chromatin targeting to transcriptional regulation: selective contact with acetylated histone H3 and H4. *F1000 Biol Rep* **1**, 98 (2009).
51. Dey, A., Chitsaz, F., Abbasi, A., Misteli, T. & Ozato, K. The double bromodomain protein Brd4 binds to acetylated chromatin during interphase and mitosis. *Proc Natl Acad Sci U S A* **100**, 8758-63 (2003).
52. Mertz, J.A. et al. Targeting MYC dependence in cancer by inhibiting BET bromodomains. *Proc Natl Acad Sci U S A* **108**, 16669-74 (2011).
53. Ott, C.J. et al. BET bromodomain inhibition targets both c-Myc and IL7R in high-risk acute lymphoblastic leukemia. *Blood* **120**, 2843-52 (2012).
54. Andersson, R. et al. An atlas of active enhancers across human cell types and tissues. *Nature* **507**, 455-61 (2014).
55. Alvarez-Dominguez, J.R. et al. Global discovery of erythroid long noncoding RNAs reveals novel regulators of red cell maturation. *Blood* **123**, 570-81 (2014).
56. Arner, E. et al. Transcribed enhancers lead waves of coordinated transcription in transitioning mammalian cells. *Science* **347**, 1010-4 (2015).
57. Fang, B. et al. Circadian enhancers coordinate multiple phases of rhythmic gene transcription in vivo. *Cell* **159**, 1140-52 (2014).
58. Lai, F., Gardini, A., Zhang, A. & Shiekhattar, R. Integrator mediates the biogenesis of enhancer RNAs. *Nature* **525**, 399-403 (2015).
59. Lam, M.T. et al. Rev-Erbs repress macrophage gene expression by inhibiting enhancer-directed transcription. *Nature* **498**, 511-5 (2013).
60. Melo, C.A. et al. eRNAs are required for p53-dependent enhancer activity and gene transcription. *Mol Cell* **49**, 524-35 (2013).
61. Yap, K.L. et al. Molecular interplay of the noncoding RNA ANRIL and methylated histone H3 lysine 27 by polycomb CBX7 in transcriptional silencing of INK4a. *Mol Cell* **38**, 662-74 (2010).
62. Devaiah, B.N. et al. BRD4 is a histone acetyltransferase that evicts nucleosomes from chromatin. *Nat Struct Mol Biol* **23**, 540-8 (2016).
63. Fujisawa, T. & Filippakopoulos, P. Functions of bromodomain-containing proteins and their roles in homeostasis and cancer. *Nat Rev Mol Cell Biol* **18**, 246-262 (2017).

64. Sanchez, R., Meslamani, J. & Zhou, M.M. The bromodomain: from epigenome reader to druggable target. *Biochim Biophys Acta* **1839**, 676-85 (2014).
65. Miller, T.C. et al. A bromodomain-DNA interaction facilitates acetylation-dependent bivalent nucleosome recognition by the BET protein BRDT. *Nat Commun* **7**, 13855 (2016).
66. Morrison, E.A. et al. DNA binding drives the association of BRG1/hBRM bromodomains with nucleosomes. *Nat Commun* **8**, 16080 (2017).
67. Ruthenburg, A.J., Li, H., Patel, D.J. & Allis, C.D. Multivalent engagement of chromatin modifications by linked binding modules. *Nat Rev Mol Cell Biol* **8**, 983-94 (2007).
68. Lauberth, S.M. et al. H3K4me3 interactions with TAF3 regulate preinitiation complex assembly and selective gene activation. *Cell* **152**, 1021-36 (2013).
69. Lauberth, S.M., Bilyeu, A.C., Firulli, B.A., Kroll, K.L. & Rauchman, M. A phosphomimetic mutation in the Sall1 repression motif disrupts recruitment of the nucleosome remodeling and deacetylase complex and repression of Gbx2. *J Biol Chem* **282**, 34858-68 (2007).

Supplementary Tables

Supplementary Table 1. shRNA targeting sequences, related to experimental procedures

Name	Sequence
sh*MMP9* eRNA-1 F	CCGGGGCTTAGAGTCTAAGCTATCTGCAGATAGCT TAGACTCTAAGCCTT TTTG
sh*MMP9* eRNA-1 R	AATTCAAAAAGGCTTAGAGTCTAAGCTATCTGCAG ATAGCTTAGACTCTA AGCC
sh*MMP9* eRNA-2 F	CCGGTACGTGAGGGTATATGCTGTTCTCGAGAACA GCATATACCCTCACG TATTTTTG
sh*MMP9* eRNA-2 R	AATTCAAAAATACGTGAGGGTATATGCTGTTCTCG AGAACAGCATATACC CTCACGTA
sh*CCL2* eRNA-1 F	CCGGCCAACACTCAGAAGCCTATCTGCAGATAGGC TTCTGAGTGTTGGTTTTTG
sh*CCL2* eRNA-1 R	AATTCAAAAACCAACACTCAGAAGCCTATCTGCAG ATAGGCTTCTGAGTGTTGG
sh*CCL2* eRNA-2 F	CCGGCCACCAAGTTCATGGTAAACTGCAGTTTACC ATGAACTTGGTGGTTTTTG
sh*CCL2* eRNA-2 R	AATTCAAAAACCACCAAGTTCATGGTAAACTGCAG TTTACCATGAACTTGGTGG
shBRD4-1 (3'UTR) F	CCGGCACGCCTTGTTACGAGCAAGTCTCGAGACTT GCTCGTAACAAGGCGTGTTTTTG
shBRD4-1 (3'UTR) R	AATTCAAAAACACGCCTTGTTACGAGCAAGTCTCG AGACTTGCTCGTAACAAGGCGTG
shBRD4-2 (exon) F	CCGGAGCTGAACCTCCCTGATTACTCGAGTAATCA GGGAGGTTCAGCTTTTTTG
shBRD4-2 (exon) R	AATTCAAAAAAGCTGAACCTCCCTGATTACTCGAG TAATCAGGGAGGTTCAGCT

Supplementary Table 2. Oligonucleotide sequences for RT-PCR analysis of gene expression, related to the experimental procedures

Name	Sequence
CSF2 eRNA-F	CTGAAGCTGTGAGCAGAGAAA
CSF2 eRNA-R	CCAAGTAGCAGGAAGAGTGATG
TNFAIP2 eRNA-F	AGGCCAAGGAGGGAGTTATAG
TNFAIP2 eRNA-R	CCTCCATTGTTGAGCAGTAGTC
MMP9 eRNA-F	TGATGGAGCTACCTCAGTG
MMP9 eRNA-R	CCACAATAGAGTTTAGCCAAGA
MMP9 mRNA-F	GACCTGGGCAGATTCCAAA
MMP9 mRNA-R	GGCAAGTCTTCCGAGTAGTTT
CCL2 eRNA-F	TTTGTGCCAGAGCCTAACC
CCL2 eRNA-R	AGTTCCCAGATCCCGTAGAA
CCL2 mRNA-F	CAGCCAGATGCAATCAATGCC
CCL2 mRNA-R	TGGAATCCTGAACCCACTTCT
CYP24A1 eRNA-F	TACGCAGTCTTTGTGCAGTAG
CYP24A1 eRNA-R	GGAGGTTACATCGCTGTTCTC
CYP24A1 mRNA-F	GTACAGCGAACTGAACAAATGG
CYP24A1 mRNA-R	CTGGAGAAGCCCAAATCTCTT
CPA4 eRNA-F	TTCTTTCTCTGGGAGCTTTCC
CPA4 eRNA-R	GTTTGGAAGCTGGACCTATGA
CPA4 mRNA-F	CAACACAATGAAGGGCAAGAA
CPA4 mRNA-R	AGGAAAGTCTGCGGCAAT
TFAP2A eRNA-F	CGCCCAGAGAAGAATGTGTTA
TFAP2A eRNA-R	GAGAAGGTGGCTAGGTTAGAGA
TFAP2A mRNA-F	AACGTTACCCTGCTCACATC
TFAP2A mRNA-R	GAGAAATTCAGCTACTGCTTTGG
MPP7 eRNA-F	GCAGACTGGAGTGTGTTTCA
MPP7 eRNA-R	ATCGCAGCGGCTTAAGAAA
MPP7 mRNA-F	CATGTGGATAGCCAGGAAGAC
MPP7 mRNA-R	ACCGGACTCTGCTTCTCATA
BRD4 mRNA-F	AAGGAAAGAGGAAGTGGAAGAG
BRD4 mRNA-R	CACATTGCTGTTGCTGCTATTA
GAPDH mRNA-F	ATTTGGTCGTATTGGGCGCCTG
GAPDH mRNA-R	AGCCTTGACGGTGCCATGGAATTT

Supplementary Table 3. Oligonucleotide sequences for ChIP analyses, related to experimental procedures

Name	Sequence
MMP9 -3.7kb enhancer-F	CAGGGTCTTGGCTAAACTCTATT
MMP9 -3.7kb enhancer-R	TGGACAGAGCTTGGCTTTC
MMP9 +2.4kb genic-F	GATGGTCCTGGGTTCTAATTCC
MMP9 +2.4kb genic-R	GCAGTTCATCCCATCTCTCATC
MMP9 +13kb -F	CGCTCTTTCTCCCTCCTAGA
MMP9 +13kb -R	TCTGGGTCAGGGCTTCT
CCL2 2.6kb enhancer-F	TTTGTGCCAGAGCCTAACC
CCL2 2.6kb enhancer-R	AGTTCCCAGATCCCGTAGAA
CCL2 +1.1kb genic-F	CAAAGAAGCTGTGATGTGAGTTC
CCL2 +1.1kb genic-R	GCACTCTCTGACTCTAGGTTTATG
CCL2 +6kb -F	ATGTCTGCCCAGCAGTATATC
CCL2 +6kb -R	ACAAGGTGGAATAGGAACAAGA

Supplementary Table 4. Oligonucleotide sequences used for cloning, related to experimental procedures

Name	Sequence
FLAG-BRD4-BD1-F	GCGGCGTCATATGAGGCAGACCAACCAA
FLAG-BRD4-BD1-R	AAGGATCCCTAGGTTTCTTCTGTGGG
FLAG-BRD4-BD2-F	GCGGCGTCATATGAAGGTCTCGGAGCAG
FLAG-BRD4-BD2-R	GCGGATCCCTAAGGCTCGTCCGGCATCTT
FLAG-BRD4-BD1/2-F	GCGGCGTCATATGAGGCAGACCAACCAA
FLAG-BRD4-BD1/2-R	GCGGATCCCTAAGGCTCGTCCGGCATCTT
His-BRD2 BD1/2-F	AAGGATCCCGAGTTACCAACCAGC
His-BRD2 BD1/2-R	AGGAATTCCTATGGTTCATCTGGCAT
His-BRD3 BD1/2-F	AAGGATCCCGCAAGACCAACCAG
His-BRD3 BD1/2-R	AGGAATTCCTAGGGCTCATCTGGCAT
His-BRD4 BD1/2-F	AAGGATCCAGGCAGACCAACCAA
His-BRD4 BD1/2-R	AGGAATTCCTAAGGCTCGTCCGGCATCTT
His-BRDT BD1/2-F	CGGGATCCCGATTGACAAATCAACT
His-BRDT BD1/2-R	AGGAATTCCTAAGGTTCAATCGGGATC
His-BRG1 BD-F	AAGGATCCTCCCCTAACCCACCCA
His-BRG1 BD-R	AGGAATTCCTAACTGTCATCCTCCTT
His-BRD7 BD-F	CGGGATCCCAGAGAAAAGATCCAA
His-BRD7 BD-R	AGGAATTCCTAATAATAAATGGTCTCTGG

Supplementary Table 5. Oligonucleotide sequences for amplification of genomic regions corresponding to various RNA species used for *in vitro* RNA synthesis, related to experimental procedures

Name	Sequence
MMP9 F	ATGGATCCATTAATACGACTCACTATAGCCCTCTCTGGCAGGTTTGGG
MMP9 R	TTGGTACCGGGAGTGCAGGCAGAGAA
CCL2 F	CCGGTACCTAATACGACTCACTATAGCTTTATCTATGAGTTGATAG
CCL2 R	TTCTCGAGAGCTTTGGAAGTTCCCAG
MEG3 F	CCGGTACCTAATACGACTCACTATAGAGGGCACTAGGAGCACGGTT
MEG3 R	TTCTCGAGCTGATGCAAGGAGAGCCC
p21 Exon2 F	CGGGTACCTAATACGACTCACTATAGGCGCCATGTCAGAACCGGCT
p21 Exon2 R	ATCTCGAGCTGTCATGCTGGTCT

Figure 1

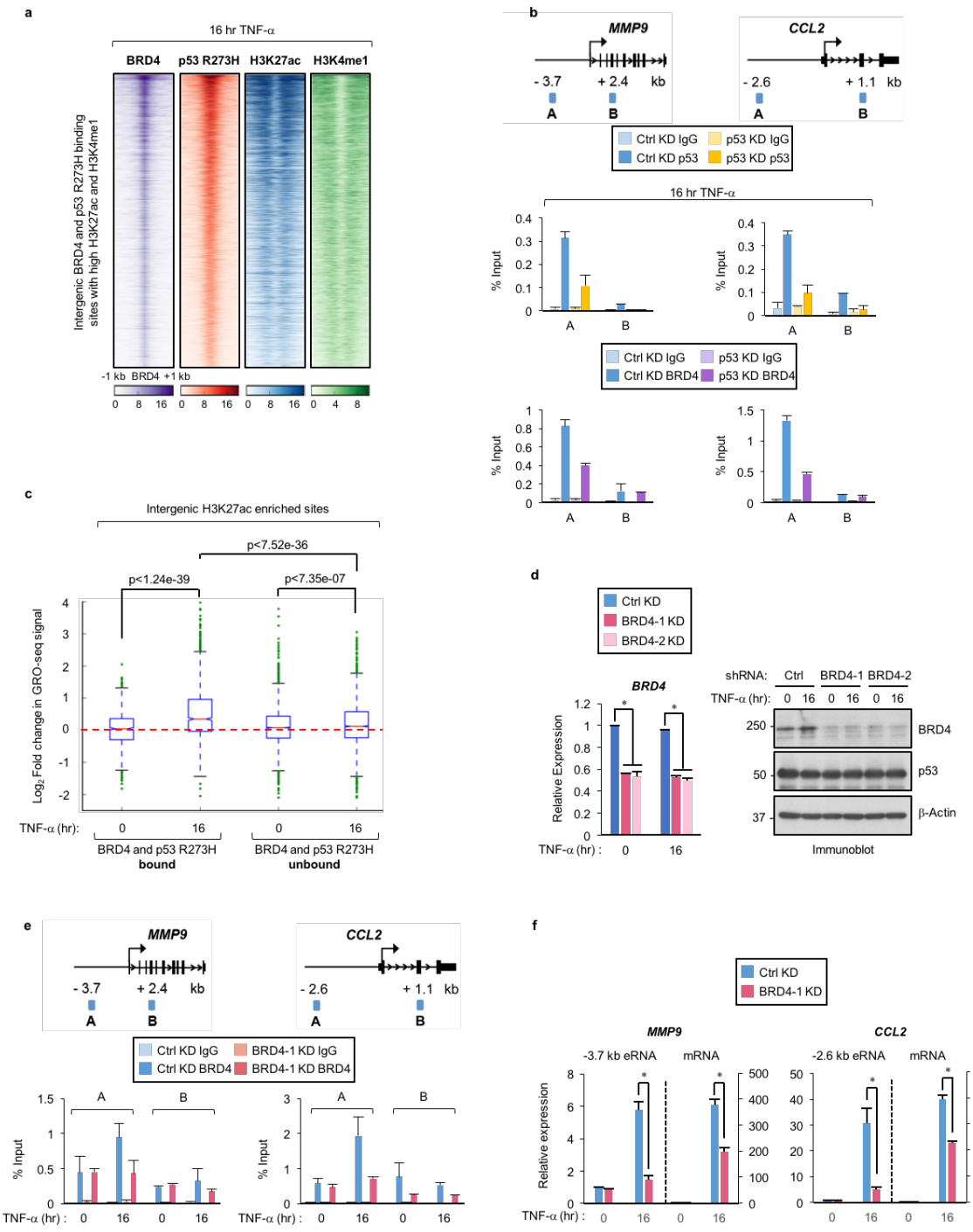

Figure 1. BRD4 co-occupies and regulates mutp53 bound enhancers in response to chronic TNF-α signaling. **a**, Heat maps of the BRD4 and p53 R273H binding sites at intergenic regions enriched for H3K27ac and H3K4me1 histone marks in SW480 cells that were treated with TNF-α for 16 hr. Each row shows ±1 kb centered on BRD4 peaks. **b**, (Top) schematics of ChIP-qPCR amplicons and (bottom) ChIP-qPCR analyses of IgG, p53 R273H, and BRD4 enrichment at the enhancer (amplicon A) and non-specific (amplicon B) regions of *MMP9* and *CCL2* gene loci in SW480 cells stably expressing LacZ (Ctrl) or p53 shRNA and treated with TNF-α for 16 hr. **c**, Boxplots showing $\log_2$ fold change in GRO-seq signal in response to TNF-α signaling at intergenic regions enriched for the H3K27ac histone mark that were co-bound or unbound by BRD4 and p53 R273H. **d**, qRT-PCR and immunoblot analysis of SW480 cells stably expressing control (Ctrl) or two different BRD4 shRNAs (BRD4-1, BRD4-2) and treated with TNF-α for 0 or 16 hr. **e**, ChIP-qPCR analysis of BRD4 binding in SW480 cells treated as described in (d) at enhancer (A) and non-specific (B) regions of *MMP9* and *CCL2* gene loci. For the ChIP-qPCR analyses in (b) and (e), the average of at least two independent experiments that are representative of three is shown with error bars denoting the standard error. **f**, qRT-PCR analyses of *MMP9* and *CCL2* eRNAs and mRNAs in SW480 cells treated as described in (d). The expression levels shown after TNF-α are relative to the levels before treatment with the bar graphs representing the average of three independent experiments and error bars denoting the standard error. Statistical significance was determined by two-tailed Student's t-test. * indicates p-value <0.05.

Figure 2

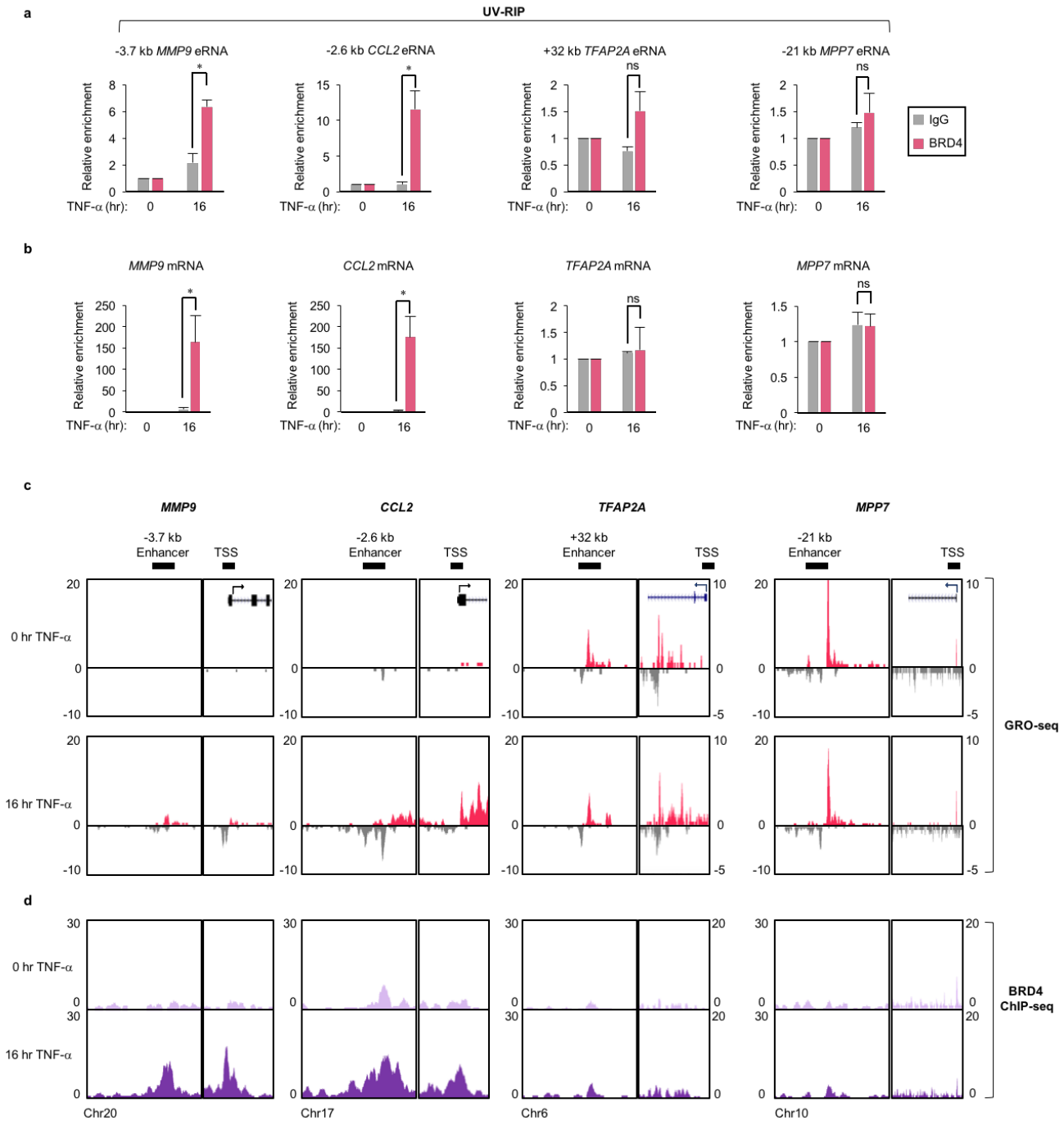

Figure 2. BRD4 associates with RNAs synthesized from genomic regions occupied by BRD4.
a, UV-RIP qPCR analysis of the *MMP9*, *CCL2*, *TFAP2A*, and *MPP7* eRNAs and **b**, mRNAs following IgG or BRD4 IP in SW480 cells treated with TNF-α for 0 or 16 hr. Enrichment levels for each TNF-α treated IP is relative to the levels before TNF-α treatment. The bar graphs represent the average of three independent UV-RIP experiments with the error bars denoting the standard error. Statistical significance was determined by two-tailed Student's t-test. * indicates p-value <0.05. ns: no significance. **c**, UCSC genome browser images of GRO-seq and **d**, BRD4 ChIP-seq signals in SW480 cells treated as described in (a) at active enhancer regions and TSSs adjacent to the *MMP9*, *CCL2*, *TFAP2A*, and *MPP7* gene loci.

Figure 3

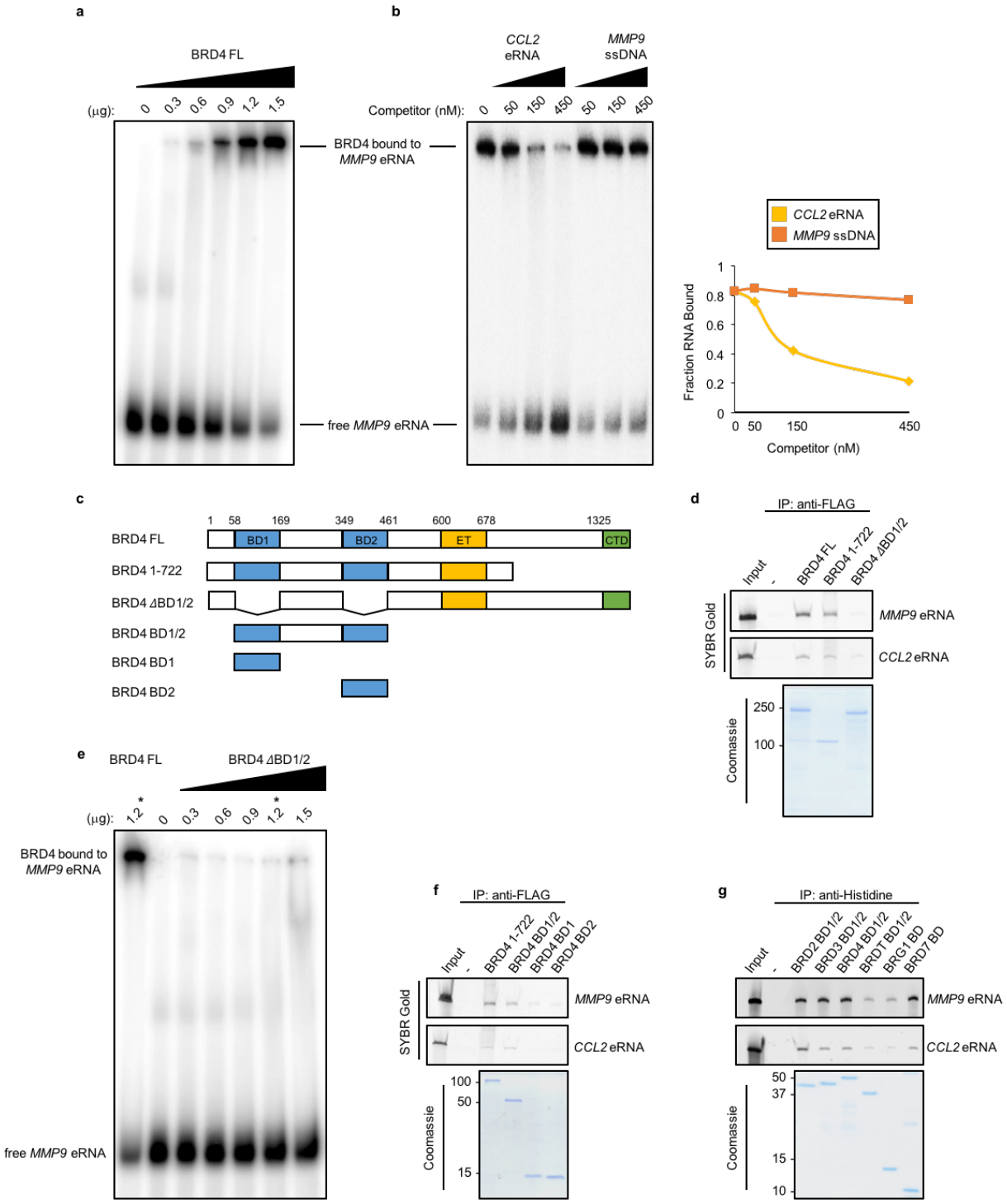

Figure 3. BRD4 directly interacts with eRNAs through its tandem bromodomains.
a, RNA EMSA performed with *in vitro* transcribed, ^{32}P-labeled *MMP9* eRNA and titrations of recombinant BRD4 FL. **b**, (Left) competition binding RNA EMSAs in which binding of ^{32}P-labeled *MMP9* eRNA to 0.9 μg of BRD4 FL was competed with 50, 150, and 450 nM unlabeled *CCL2* eRNA and *MMP9* ssDNA. (Right) quantification of the fraction of RNA bound to BRD4 FL in the presence of unlabeled competitors as denoted, corresponding to the autoradiogram shown in the left panel. **c**, Schematic of BRD4 proteins expressed, purified, and used in RNA EMSA and *in vitro* RNA binding assays. **d**, **f**, *In vitro* pull-down of *MMP9 and CCL2* eRNAs with the indicated FLAG-tagged BRD4 proteins and **g**, the His-tagged tandem BDs of BRD2, BRD3, BRD4, and BRDT and the single BDs of BRG1 and BRD7 as revealed by SYBR Gold staining and SDS-PAGE/coomassie staining analyses of the purified proteins. **e**, RNA EMSA performed with *in vitro* transcribed ^{32}P-labeled *MMP9* eRNA and titrations of recombinant BRD4 ΔBD1/2. One reaction with 1.2 μg of BRD4 FL was also performed as control and denoted with *. **f**, All RNA EMSAs and *in vitro* binding assays were performed three independent times with representative images for each assay shown in the corresponding panels.

Figure 4

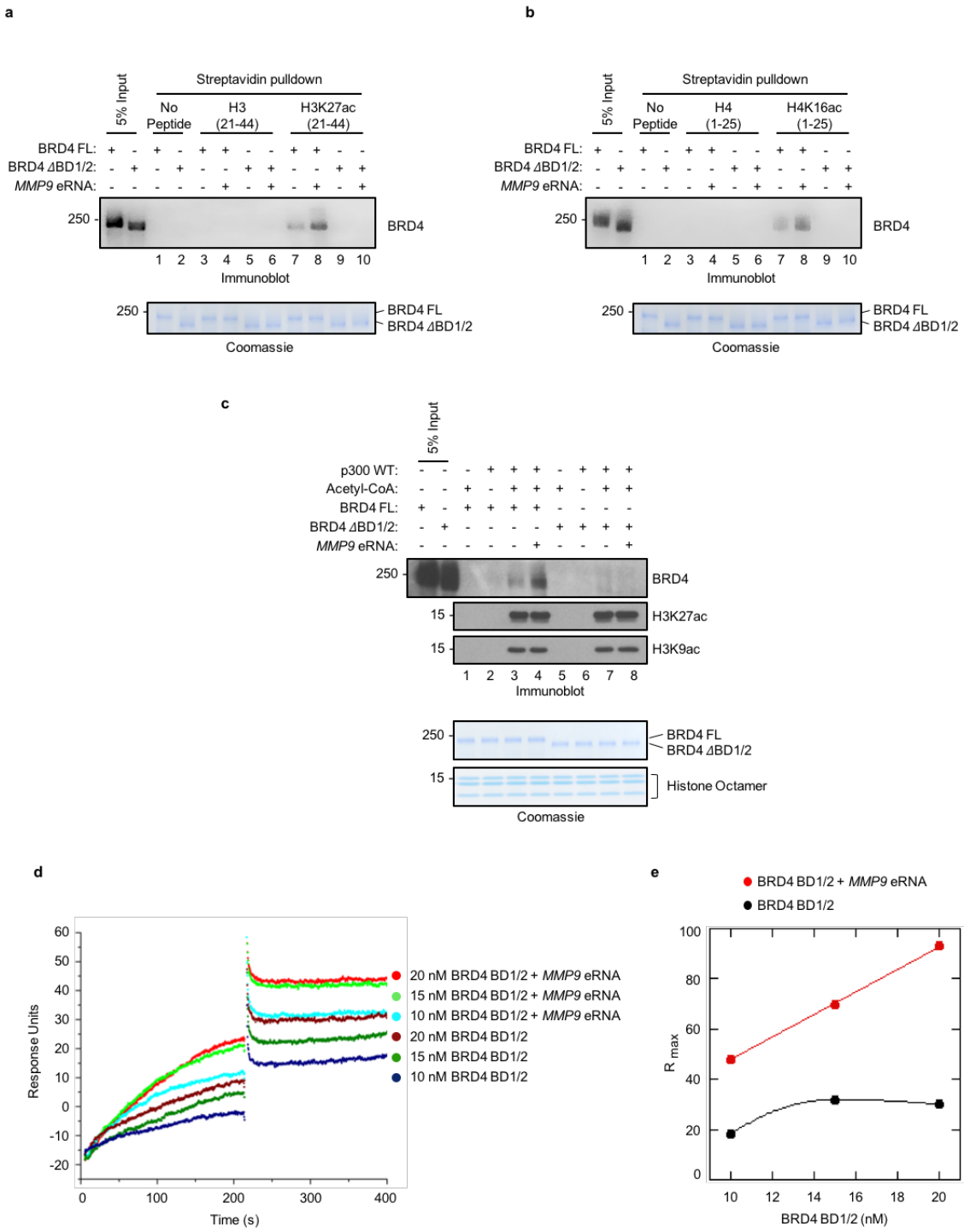

Figure 4. eRNAs cooperate with acetylated histones to enhance BRD4 binding, *in vitro*.
Immobilized peptide pulldown assay using biotinylated **a**, H3 peptides (unmodified or K27acetylated-modified) and **b**, H4 peptides (unmodified or K16acetylated-modified) with either recombinant BRD4 FL or BRD4 Δ**BD1/2** in the absence or presence of refolded *MMP9* eRNA as indicated. Recombinant BRD4 FL and BRD4 Δ**BD1/2** were detected by immunoblotting with an antibody specific to BRD4. **c**, Immunoblot analysis of *in vitro* binding assays with unacetylated or acetylated histone octamers, recombinant BRD4 FL or Δ**BD1/2**, and refolded *MMP9* eRNA as indicated. Immunoblot analysis with H3K27ac and H3K9ac antibodies confirmed the p300- and acetyl-CoA-mediated acetylation of the histone octamers. Lower panels in (a), (b), and (c) represent the loading of the indicated proteins by coomassie staining. **d**, Analysis of BRD4 BD1/2 binding to immobilized, biotin-labeled H3K27ac peptides in the absence or presence of refolded *MMP9* eRNA as measured in response unit (RU) by surface plasmon resonance. Representative sensorgrams were obtained from injections of 10, 15, and 20 nM of BRD4 BD1/2 with and without 0.2 nM of *MMP9* eRNA in binding buffer for 300 s at 50 μl min^{-1}. **e**, R_{max} plot depicting the maximal binding capacity of BRD4 BD1/2 at various concentrations in the absence (black) and presence (red) of refolded *MMP9* eRNA. All *in vitro* binding assays were performed three independent times with representative images for each assay shown in the corresponding panels.

Figure 5

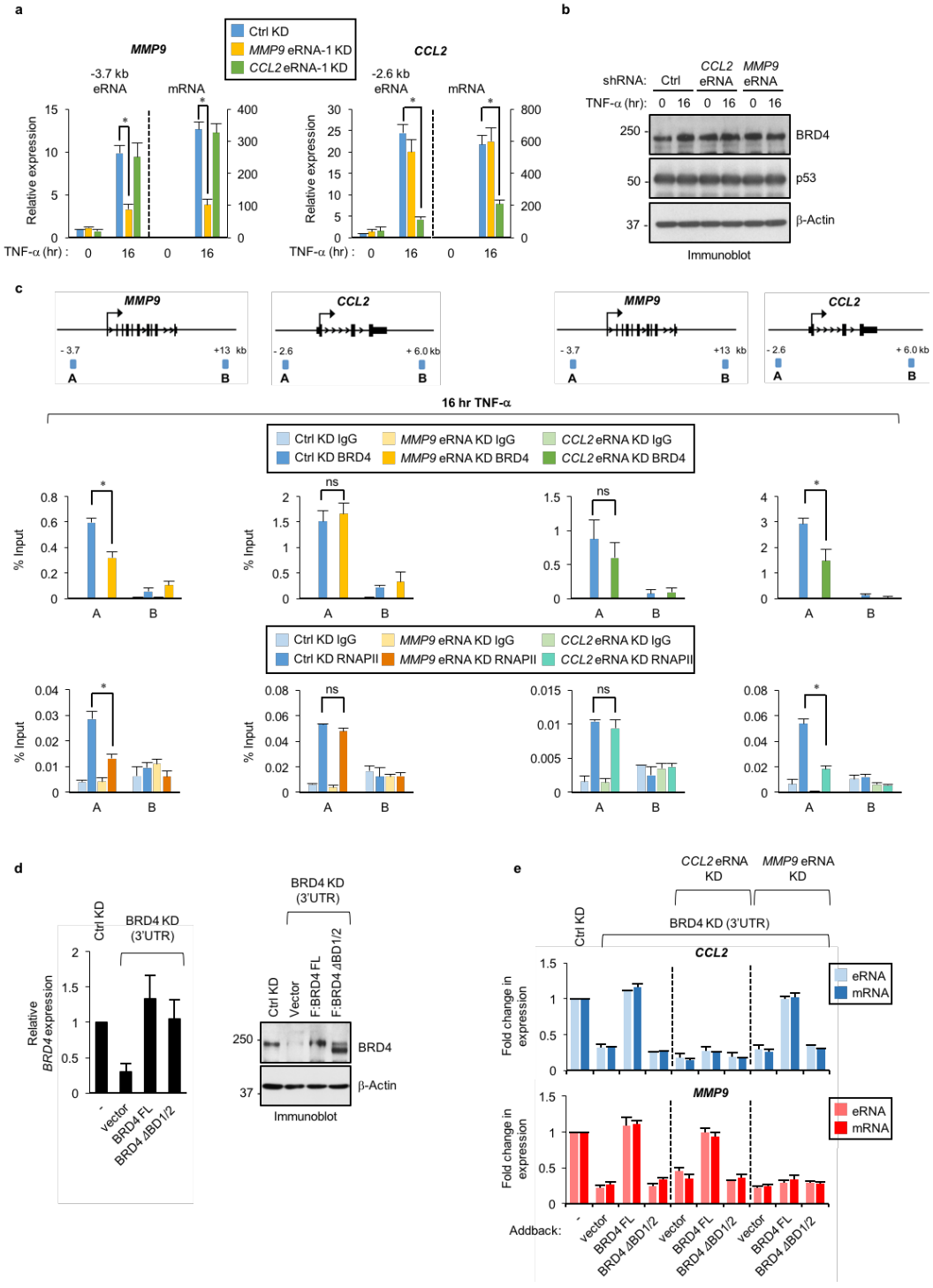

Figure 5. BRD4 enhancer occupancy and regulation of select eRNAs and genes is modulated by BRD4 interactions with eRNAs.

a, qRT-PCR analysis of *MMP9* and *CCL2* eRNAs and mRNAs and **b**, immunoblot analysis of SW480 cells stably expressing control (Ctrl) or *MMP9* and *CCL2* eRNA shRNAs and treated with TNF-α for 0 or 16 hr. **c**, IgG, BRD4, and RNAPII ChIP-qPCR analyses at the enhancers (A) and nonspecific (B) regions of *MMP9* and *CCL2* gene loci in SW480 cells described in (a) and treated with TNF-α for 16 hr. The average of at least two independent ChIP experiments that are representative of three is shown with error bars denoting the standard error. **d**, qRT-PCR and immunoblot analysis of BRD4 mRNA and protein levels in SW480 cells that expressed control or BRD4 shRNAs together with empty vector control or shRNA-resistant plasmids expressing BRD4 FL or BRD4 ΔBD1/2 and treated with TNF-α for 16 hr. **e**, qRT-PCR analysis of *MMP9* and *CCL2* eRNA and mRNA expression levels in single BRD4 or double BRD4 and *MMP9* or *CCL2* eRNA knockdown SW480 cells that were transiently transfected with shRNA-resistant constructs expressing BRD4 FL or BRD4 ΔBD1/2 and treated with TNF-α for 16 hr. For all eRNA and mRNA expression analyses in (a), (d), and (e), the expression levels following TNF-α treatment are relative to the levels before TNF-α and bar graphs represent the average of three independent experiments with the error bars denoting the standard error. Statistical significance was determined by two-tailed Student's t-test. * indicates p-value <0.05. ns: no significance.

Figure 6

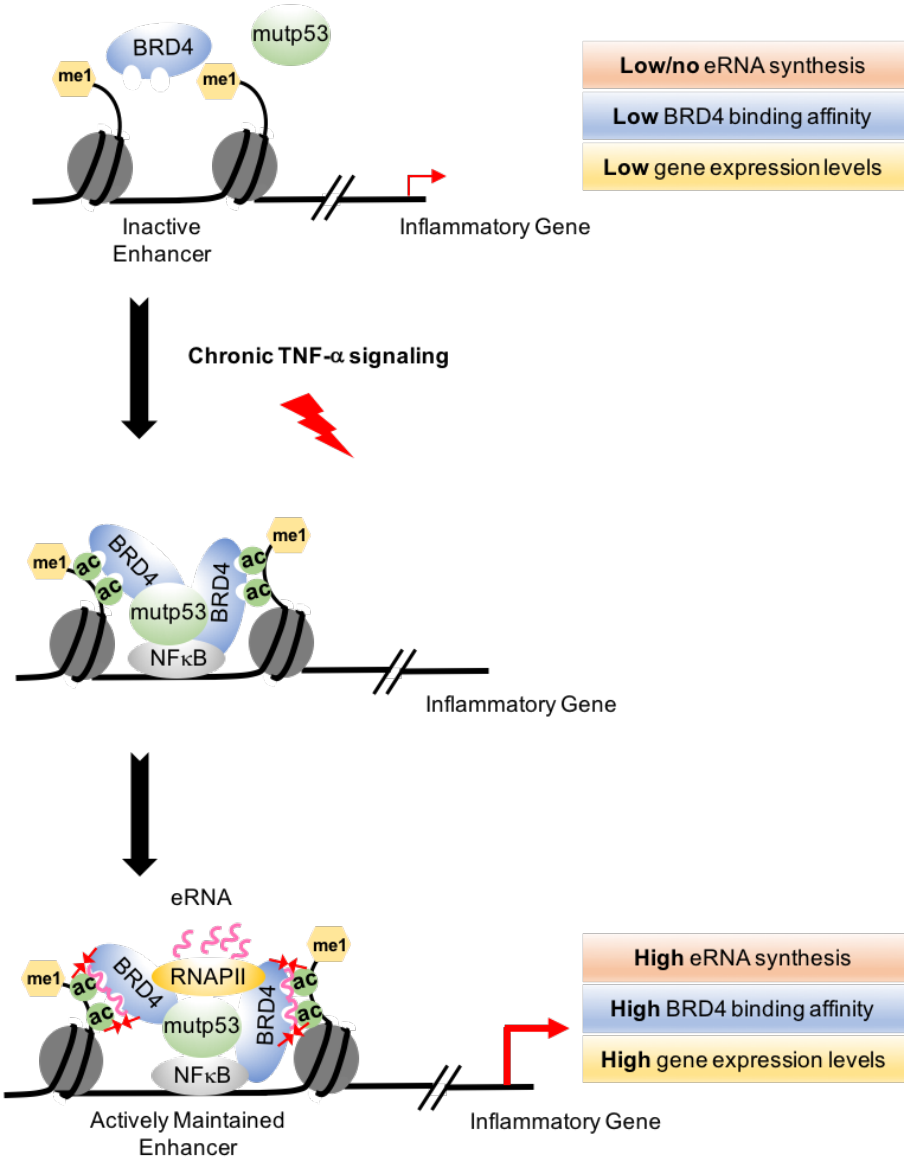

Figure 6. Proposed model for eRNA-mediated BRD4 tethering to acetylated histones at active enhancers. Upon chronic TNF-α signaling, NFκB recruits mutp53 to a subset of enhancers as we have previously described[48]. In our current study, we show that BRD4 is also recruited to these mutp53-activated enhancers following chronic immune signaling. Subsequently, eRNAs synthesized from the activated enhancers bind to the bromodomains of BRD4 to enhance its binding to acetylated chromatin. This stabilization of BRD4 at active enhancers contributes to TNF-α-induced production of eRNAs and potent expression of the nearby tumor promoting genes.

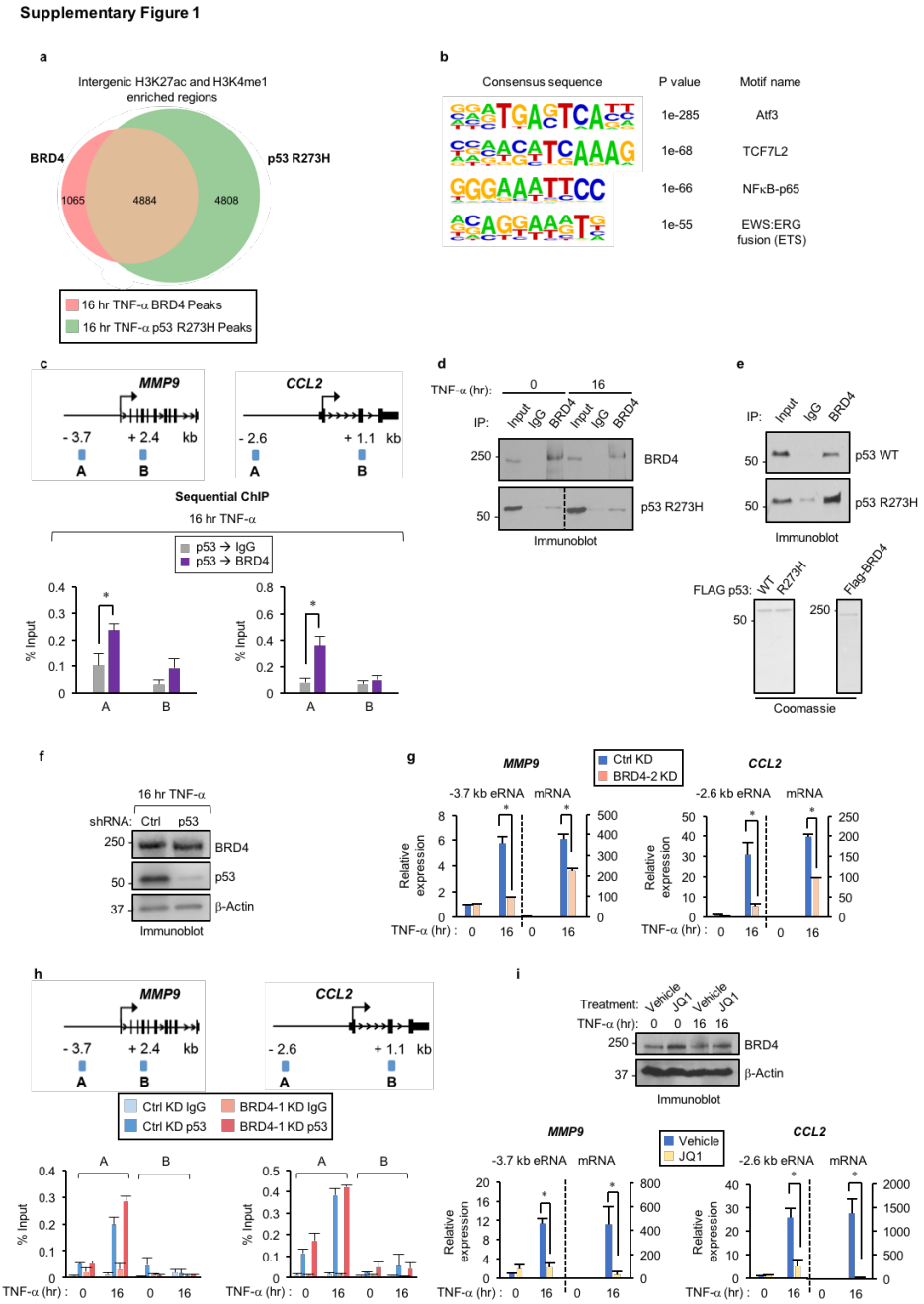

Supplementary Figure 1. BRD4 cooperates with mutp53 at active enhancers to regulate enhancer and gene activation upon chronic immune signaling.

a, Venn diagram depicting the overlap between p53 R273H and BRD4 binding sites at H3K27ac and H3K4me1 enriched, intergenic regions in SW480 cells after 16 hr TNF-α treatment. **b**, *De novo* motif analyses of the BRD4 and p53 R273H co-bound ChIP-seq peaks at active enhancer regions. **c**, (Top) schematics of ChIP-qPCR amplicons and (bottom) ChIP-qPCR analysis of sequential ChIP with p53 antibody followed by BRD4 and control IgG antibody in SW480 treated with TNF-α for 16 hr at the enhancer (A) and nonspecific (B) regions of *MMP9* and *CCL2* gene loci. **d**, Immunoblot analysis of BRD4 Co-IP performed with lysates from SW480 cells treated with TNF-α for 0, 16 hr with indicated antibodies. **e**, (Top) immunoblot analysis of direct interaction assay between BRD4 and p53 (wild-type and R273H) using (bottom) recombinant proteins analyzed by SDS-PAGE and coomassie staining. Co-IP and binding assays were performed three independent times with representative images for each assay shown in the corresponding panels. **f**, Immunoblot analysis of SW480 cells stably expressing LacZ (Ctrl) or p53 shRNA and treated with TNF-α for 0 or 16 hr with the indicated antibodies. **g**, qRT-PCR analysis of *MMP9* and *CCL2* eRNAs and mRNAs in SW480 cells stably expressing control (Ctrl) or a second BRD4 shRNA oligo (BRD4-2) and treated with TNF-α for 0 or 16 hr. **h**, ChIP-qPCR analysis of IgG and p53 R273H enrichment at the enhancer (A) and nonspecific (B) regions of *MMP9* and *CCL2* gene loci in SW480 cells stably expressing control or BRD4 shRNA and treated with TNF-α for 0 or 16 hr. **i**, Immunoblot (top) and qRT-PCR analysis (bottom) of SW480 cells treated with vehicle (DMSO) or JQ1 and TNF-α for 0 or 16 hr. In (g) and (i) the expression levels following TNF-α treatment are relative to the levels before TNF-α exposure and bar graphs represent the average of three independent experiments with the error bars denoting the standard error. In (c) and (h) the average of at least two independent ChIP experiments that are representative of three is shown with error bars denoting the standard error. Statistical significance was determined by two-tailed Student's t-test. * indicates p-value <0.05.

Supplementary Figure 2

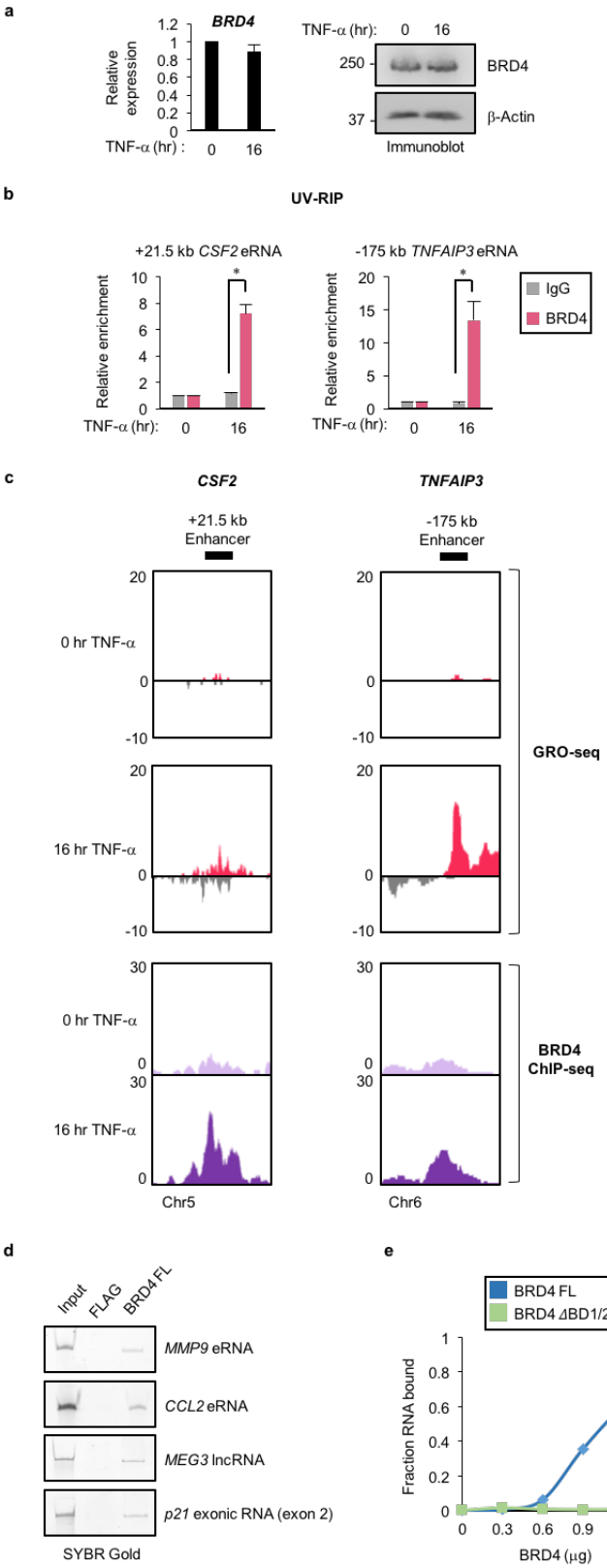

Supplementary Figure 2. BRD4 directly interacts with RNAs.

a, qRT-PCR and immunoblot analyses of SW480 cells treated with TNF-α for 0 or 16 hr. **b**, UV-RIP qPCR analysis of the *CSF2* and *TNFAIP3* eRNAs following IgG or BRD4 IP in SW480 cells treated with TNF-α for 0 or 16 hr. Enrichment levels for each TNF-α treated IP is relative to the levels before TNF-α treatment. The bar graphs represent the average of three independent UV-RIP experiments with the error bars denoting the standard error. Statistical significance was determined by two-tailed Student's t-test. * indicates p-value <0.05. **c**, UCSC genome browser images of GRO-seq and BRD4 ChIP-seq signals in SW480 cells treated as described in (a) at active enhancer regions of *CSF2* and *TNFAIP3*. **d**, SYBR Gold staining of *in vitro* binding assay between BRD4 FL and various *in vitro* transcribed RNA molecules. Three independent *in vitro* binding assays were performed. **e**, Quantification of RNA EMSAs to determine the fraction of RNA bound to BRD4 FL as shown in Fig. 3a and BRD4 ΔBD1/2 as shown in Fig. 3e.

Supplementary Figure 3

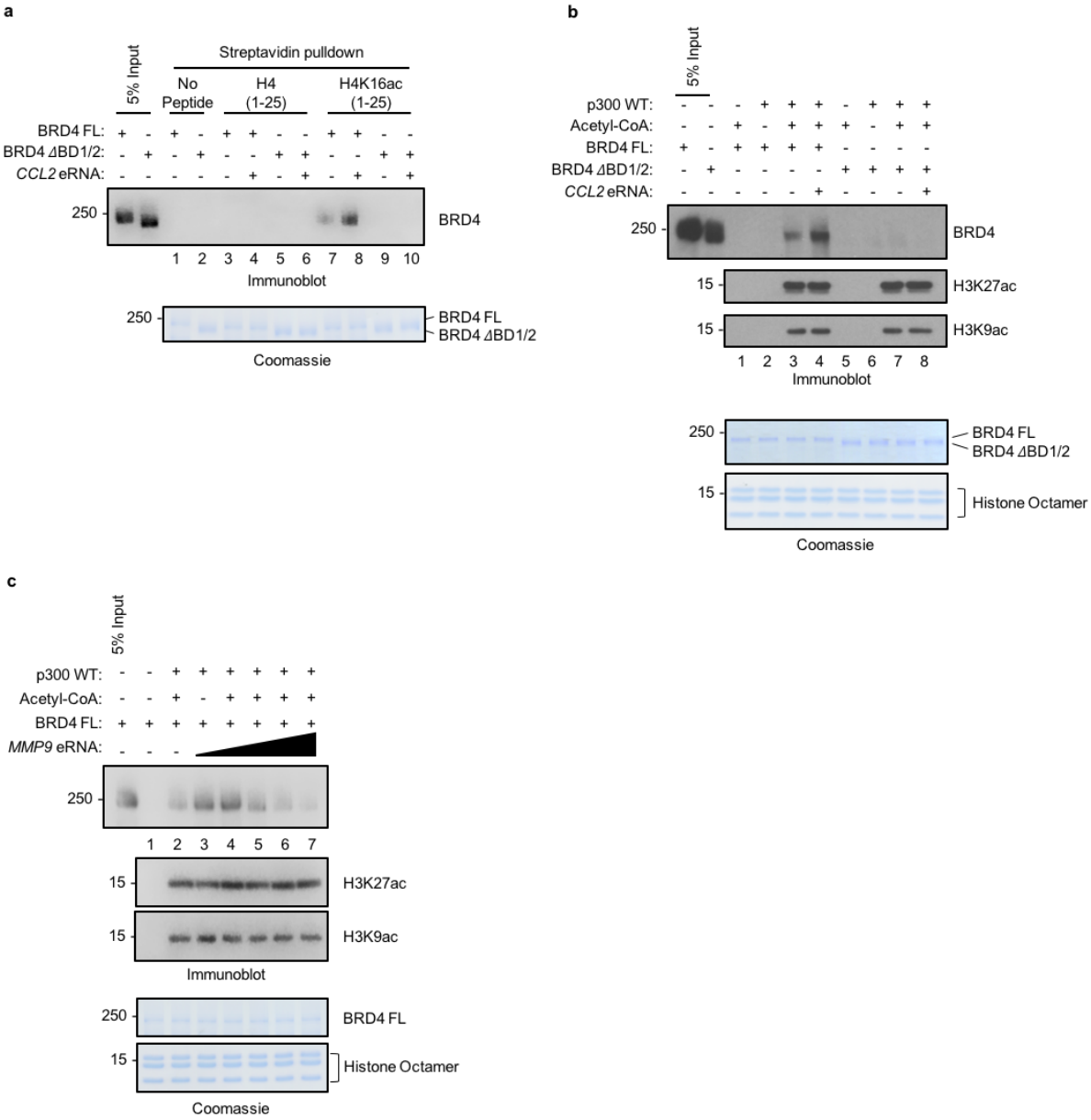

Supplementary Figure 3. eRNAs enhance BRD4 binding to acetylated histone peptides and octamers *in vitro.* **a,** Immobilized peptide pulldown assay using biotinylated H4 peptides (unmodified or K16acetylated-modified) with either recombinant BRD4 FL or BRD4 ΔBD1/2 in the absence or presence of refolded *CCL2* eRNA as indicated. Recombinant BRD4 FL and BRD4 ΔBD1/2 were detected by immunoblotting with an antibody specific to BRD4. **b,** Immunoblot analysis of *in vitro* binding assays with unacetylated or acetylated histone octamers, recombinant BRD4 FL or ΔBD1/2, and refolded *CCL2* eRNA as indicated. **c**, *In vitro* histone octamer binding assay as described in (b) with recombinant BRD4 FL and increasing doses of refolded *MMP9* eRNA (0.06, 0.1, 0.2, 1, and 2 nM). In (b) and (c), immunoblot analysis with H3K27ac and H3K9ac antibodies confirmed the p300- and acetyl-CoA-mediated acetylation of the histone octamers. Lower panels in (a), (b), and (c) represent the loading of the indicated proteins by coomassie staining. All *in vitro* binding assays were performed three independent times.

Supplementary Figure 4

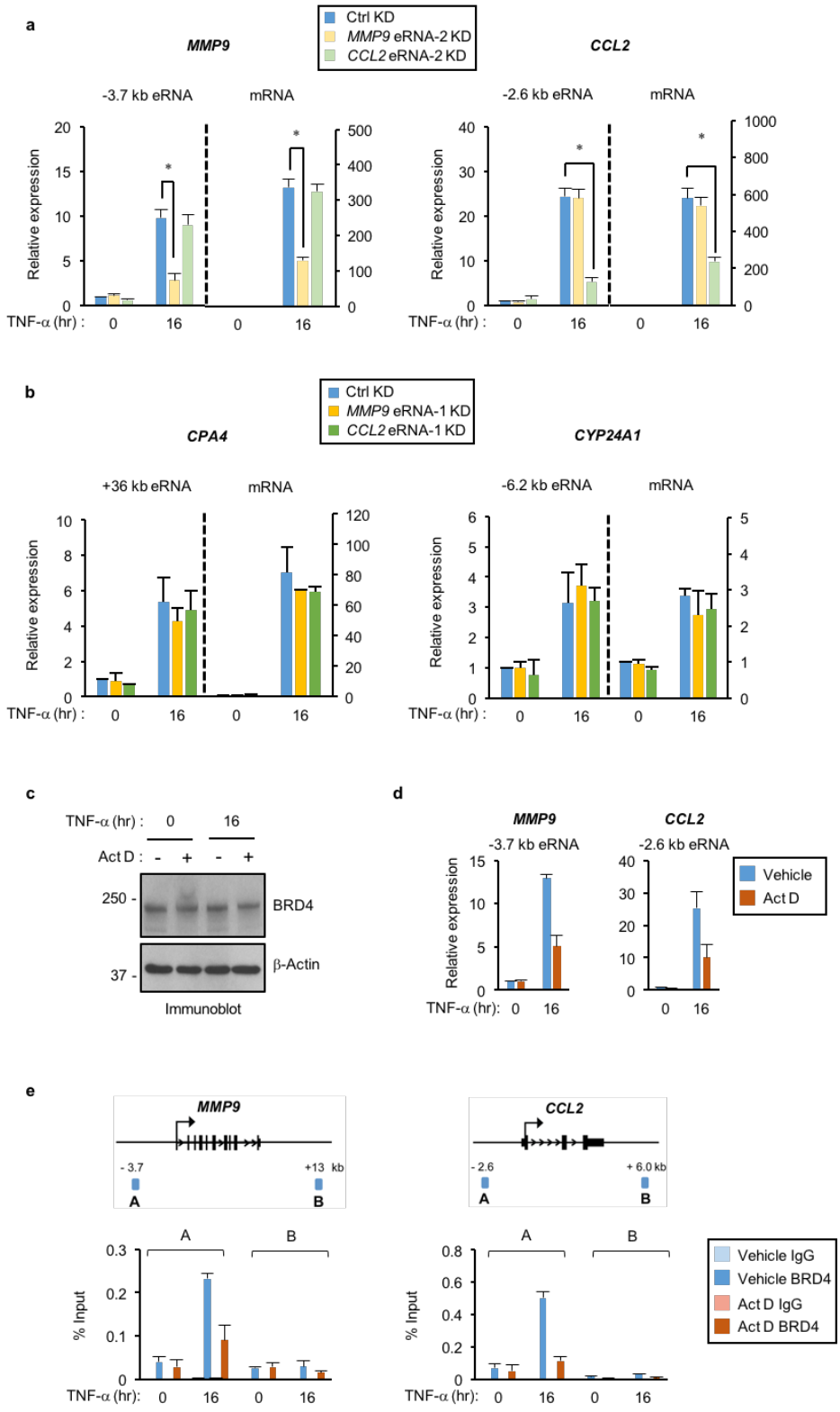

Supplementary Figure 4. eRNA depletion reduces the expression of corresponding mRNAs and impacts BRD4 binding.

a, qRT-PCR analysis of *MMP9* and *CCL2* eRNAs and mRNAs in SW480 cells expressing control or a second shRNA oligo against *MMP9* and *CCL2* eRNAs and treated with TNF-α for 0 or 16 hr. **b**, qRT-PCR analysis of *CPA4* and *CYP24A1* eRNA and mRNAs in SW480 cells treated as described in Fig. 5a. **c**, Immunoblot and **d**, qRT-PCR analysis of SW480 cells treated with TNF-α for 0 or 16 hr and treated with Actinomycin D for 2 hr. In (a), (b), and (c), the expression levels following TNF-α treatment are relative to the levels before TNF-α exposure. The bar graphs represent the average of three independent experiments. **e**, ChIP-qPCR analyses of IgG and BRD4 enrichment in SW480 cells treated as described in (c), at the enhancer (A) and nonspecific (B) regions of *MMP9* and *CCL2* gene loci. An average of two independent ChIP experiments that are representative of three is shown with error bars denoting the standard error.